Preprint typeset in JHEP style - HYPER VERSION

TAUP-2876/08
June 29, 2008

Inclusive gluon production in the dipole approach: AGK cutting rules.

Eugene Levin * **and Alex Prygarin** †

Department of Particle Physics, School of Physics and Astronomy
Raymond and Beverly Sackler Faculty of Exact Science
Tel Aviv University, Tel Aviv, 69978, Israel

Abstract: We consider single gluon production in the dipole model and reproduce the result of Kovchegov and Tuchin for the adjoint (gluonic) dipole structure of the inclusive cross section. We show the validity of the adjoint dipole structure to any order of evolution deriving and solving the non-linear evolution for the non-diagonal cross section of a dipole scattering off the target. The form of the solution to this equation restores the dipole interpretation for non-diagonal cross sections, that appear in gluon production. Using this formalism, we analyse the single inclusive production cross section in terms of the contributions of different multiplicities, and we derive the Abramovskii-Gribov-Kancheli(AGK) cutting rules for two Pomeron exchange. The cutting rules, which were found in this formalism, fully reproduce the original AGK rules for the total cross section. However, for the case of gluon production, the AGK rules are violated already for one gluon emission from the vertex.

Keywords: Colour dipole model, inclusive production, jet production, BK equation, BFKL equation.

*leving@post.tau.ac.il, levin@mail.desy.de;
†prygarin@post.tau.ac.il

Contents

1. Introduction

The high energy scattering in the perturbative QCD has been extensively studied during the last two decades. Special interest is drawn to the situation where the scattering amplitude unitarizes, which is called a saturation regime[1, 2, 3]. In this regime the density of partons becomes so high that one cannot ignore their mutual interactions anymore. A very convenient framework for studying parton saturation is the so-called dipole approach [4], where the size of the elementary degree of freedom, namely, dipole is assumed to be much smaller than $1/\Lambda_{QCD}$ justifying the use of perturbative QCD. A lot of observables were calculated using this extremely convenient formalism. In the present paper we consider the Abramovsky-Gribov-Kancheli (AGK) [5] cutting rules in the framework of the dipole approach. The AGK cutting rules allow us to expand the dipole approach for the calculation of the scattering elastic amplitude (total cross section) to the consideration of exclusive processes such as diffractive production [6] and different correlations in multiparticle production processes. They lead also to a better understanding of the

k_t-factorization in the region of low $x_{Bjorken}$ where the new momentum scale: saturation momentum, makes this factorization questionable. Being such an important tool, the AGK cutting rules have been discussed in QCD (see Refs. [7]), but the recent study of the inclusive cross section in QCD has drawn a new attention to these rules. The project was started by Kovchegov [8] and Kovchegov and Tuchin [9] for the single inclusive cross section and it was extended to the case of the double gluon production by Kovchegov and Jalilian-Marian [10]. The main result of this study could be summarized as follows: for the single inclusive cross sections the k_t-factorization has been proved which leads to a plausible validity of the AGK cutting rules while in the case of the double inclusive cross section the explicit violation of the AGK cutting rules has been found.

The result of Refs. [8, 9] for the single inclusive cross sections was confirmed afterwards by Braun [11] using the reggeized gluon technique, as well as, by Marquet [12] and Kovner and Lublinsky [13] in the Wilson lines formalism.

The result of Ref. [10] was strongly questioned by Braun [11], who claimed that one of the gluons (upper) is necessarily emitted from the vertex and such a contribution cannot represent a genuine violation of the AGK cutting rules, because the original derivation of the AGK rules was based on the assumption that there are no emissions from vertices.

Motivated by this discrepancy in the results, we revisited first the single inclusive case and found that the result of Kovchegov and Tuchin is correct. In Section 2 we discuss the key problem of real-virtual cancellation which is the essential question for approaching the AGK cutting rules problem in QCD. Indeed, the key question for everybody and the nightmare of everybody who is interested in the AGK cutting rules is whether the set of diagrams that contribute to the total cross section, and to the inelastic production is the same. In this section as well as in the sections 2-4 we complete the analysis, started by Chen and Mueller [14] and by Kovchegov and Tuchin[8, 9], of the set of diagrams that are responsible for the total and inelastic cross sections.

In Section 3 and Section 4 we repeat the Kovchegov and Tuchin analysis of the single inclusive production but introducing a new function $M\left(jk|ik\right)$ in which it is easy to separate elastic and inelastic interaction. We obtain a new non-linear evolution equation and solve it. Function $M\left(jk|ik\right)$ describes the non-diagonal process of scattering of dipole with size $r_{jk}=|x_j-x_k|$ off the target with transition of this dipole to the dipole of the size $r_{ik}=|x_i-x_k|$. At first sight such an amplitude contradicts the key idea of the dipole approach: dipoles are correct degrees of freedom at high energy or, in other words, the interaction matrix is diagonal with respect to the sizes of the interacting dipoles. We show by solving the evolution equation for $M\left(jk|ik\right)$, that the dipole approach survives this test of existence the non-diagonal amplitudes at high energy.

Starting from Section 5 we consider the AGK cutting rules. The AGK cutting rules give us the relation between the total cross section at high energy and the processes of multiparticle production. The main idea stems from the unitarity constraint for the BFKL Pomeron [15] which describes the high energy scattering amplitude in the leading log $(1/x_{Bjorken})$ approximation of perturbative QCD. The unitarity reads as

$$2N\left(Y;x,y\right) \;=\; |N\left(Y;x,y\right)|^2+G_{in}\left(Y;x,y\right) \tag{1.1}$$

where $Y=(1/x)$ and (x,y) are the coordinates of the incoming dipole; $N\left(Y;x,y\right)$ is the imaginary part of the elastic amplitude and the first term describes the elastic scattering (assuming that the real part of the amplitude is small at high energy) while the second stands for the contribution of all inelastic processes. In the leading log $(1/x_{Bjorken})$ approximation the elastic contribution can be neglected and for the BFKL Pomeron Eq. (1.1) can be reduced to the form (see Fig. 1):

$$2N^{BFKL}\left(Y;x,y\right) \;=\; G^{BFKL}_{in}\left(Y;x,y\right) \tag{1.2}$$

In what follows we call $G_{in}\left(Y;x,y\right)$ a cut Pomeron while $N^{BFKL}\left(Y;x,y\right)$ will be called a Pomeron or uncut Pomeron.

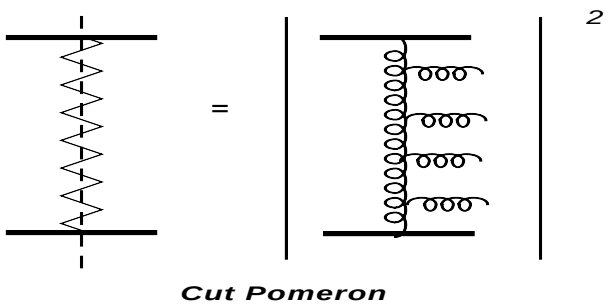

Figure 1: The definition of cut Pomeron through the BFKL ladder.

In this paper we prove the AGK cutting rules for the case of the totally inclusive processes (see Fig. 2). We show that the same set of the diagrams determine the total cross section and the processes of the inelastic production. Therefore, each inelastic contribution for the exchange of two BFKL Pomerons can be calculated in terms of the elastic amplitude with the coefficients shown in Fig. 2. The situation changes drastically for the case when we measure one extra particle (see Fig. 3. In this case the inelastic production stems from different set of the diagrams than the total cross section and we do not have the simple expression for each inelastic processes through the elastic amplitude as well as we do not find the simple relations between different processes.

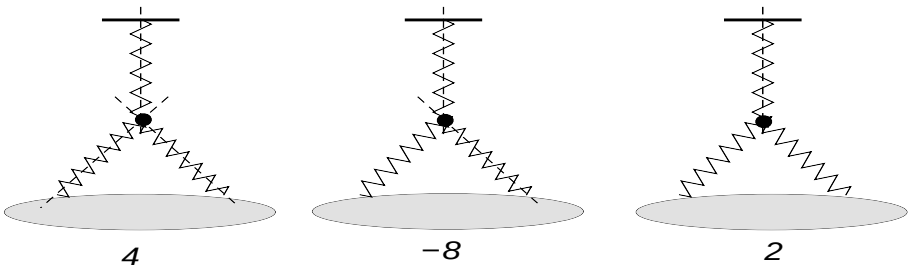

Figure 2: The AGK cutting rules for the total inclusive processes. Cut Pomeron is defined in Fig. 1 and in Eq. (1.2).

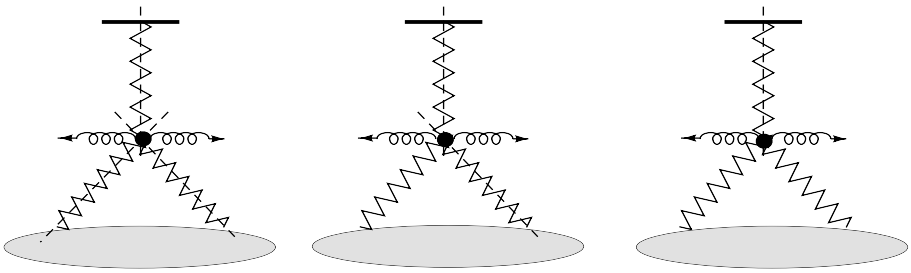

Figure 3: Violation of AGK cutting rules for the processes with additional emission of one particle (gluon). Cut Pomeron is defined in Fig. 1 and in Eq. (1.2).

In the Appendices we adduce some calculations relevant to our discussion.

2. Real-virtual cancellations

In this section we briefly review the main result of Ref. [14] with a special emphasis on so-called real-virtual cancellations. These cancellations play an important role in the derivation of both BFKL [15] and BK [17, 18] equations in the colour dipole model. Let us consider a colourless onium state with one extra soft gluon emission. The soft gluon

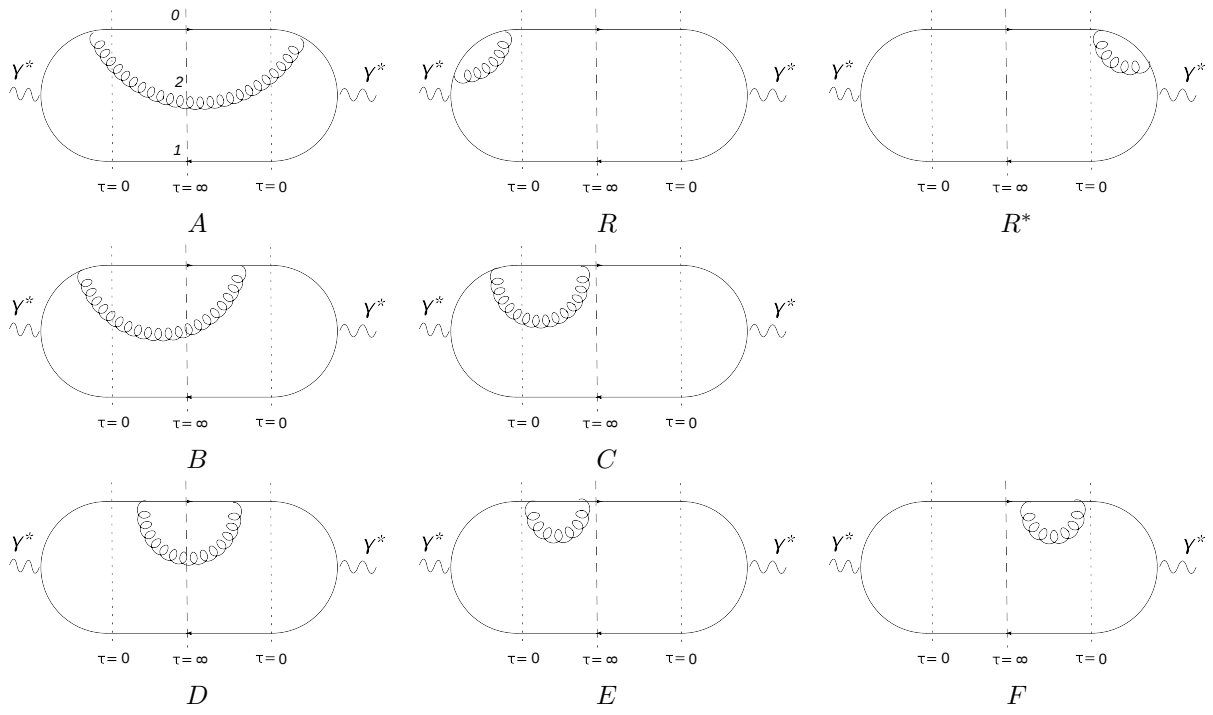

Figure 4: All possible emissions of a soft gluon in the onium state, diagrams B^* and C^* are not shown.

can be emitted either from a quark or from a antiquark lines. For simplicity we consider here only the emissions from the antiquark line. We assign the transverse coordinates x_1, x_0 and x_2 to the quark, antiquark and soft gluon lines, respectively. The system interacts with the target by instantaneous interaction via Coulomb gluon exchange. We use an eikonal approximation allowing for multiple interaction with the target. It was shown by Kovchegov [8] that there are no soft gluon emissions during the interaction time so that the eikonal rescattering can be regarded as an instantaneous as well. To avoid any question regarding the use of the eikonal approximation as the initial condition for the evolution at low energy, we consider the interaction with heavy nuclei for which the eikonal formula, as well as, the non-linear evolution equation in the mean field approximation (Balitsky-Kovchegov (BK) equation [17, 18]) are proved. We work in Light Cone Perturbation Theory (LCPT)[19] with light-cone gauge and denote by $\tau = 0$ the interaction time while the detector that measures the particles in the final state is placed at $\tau = \infty$.

For simplicity, we consider only soft gluon emissions from the antiquark with coordinate x_0. The relevant diagrams are shown in Fig. 4

In diagram A of Fig. 4 the soft gluon at x_2 is emitted before the interaction time in both amplitude and conjugate amplitude. In diagrams R and R^* the soft gluon is emitted and absorbed before the interaction time, these diagrams give reggeization term of the BFKL and BK equations in the dipole model. Only diagrams A, R and R^* are present in the BFKL[15] and BK [17, 18] equations, all other diagrams are canceled as we will show shortly. This cancellation is called real-virtual cancellation, where any real emission (absorption) of the soft gluon after time $\tau = 0$ is canceled by its virtual counterpart(s). Namely, let us consider diagrams B and C where the soft gluon is emitted before the interaction time in the amplitude, but not in the conjugate amplitude. The emitted gluon be either present or not in the final state at $\tau = \infty$. As it was shown in Ref. [14] (see also Appendix A for more details) those diagrams differ only by a minus sign and thus cancel each other in the total cross section (same for B^* and C^*, not shown

here). Similar cancellation happens also to D, E and F, but one should note that E and F have a factor of $\frac{1}{2}$ w.r.t. diagram D due to a light-cone time ordered integral as shown in Appendix of Ref. [14].

Thus we are left with diagrams A, R and R^*. To this we should add also diagrams with the soft gluon emission from the quark line at x_1, which translates into the BFKL kernel in the dipole model, namely, $\left(\frac{x_{12}}{x_{12}^2} - \frac{x_{02}}{x_{02}^2}\right)^2 = \frac{x_{10}^2}{x_{12}^2 x_{20}^2}$.

In Section 4 we present the derivation of BK equation in more general case and show how this reduces to well-known equation

$$\frac{\partial N(10)}{\partial y} = \frac{\bar{\alpha}_s}{2\pi} \int d^2x_2 \frac{x_{10}^2}{x_{12}^2 x_{20}^2} \{N(12) + N(02) - N(10) - N(12)N(02)\} \tag{2.1}$$

with $N(10) = \mathrm{Im}A_{el}(x_1, x_0; Y)$ being the imaginary part [1] of the elastic scattering amplitude of a colourless dipole with quark and antiquark coordinates at x_1 and x_0 ($\vec{x}_{10} = \vec{x}_1 - \vec{x}_0$), respectively.

3. Inclusive one gluon production: no evolution included

In this section we follow the lines of Ref. [8] in the derivation of the single gluon inclusive production cross section in DIS with no evolution included. However, in our derivation we treat separately all the contributions that sum into the final result of Ref. [8]. The reason for that is our goal to include properly the evolution in the inclusive cross section for one gluon production as will be clarified in Section 4.

The general expression for the gluon production cross section in DIS is given by

$$\frac{d\sigma^{\gamma^* A \to GX}}{d^2k\, dy} = \frac{1}{2\pi^2} \int d^2x_{10}\, dz |\psi^{\gamma^* \to q\bar{q}}(x_{01}, z)|^2 \frac{d\sigma^{q\bar{q}A \to GX}(x_1, x_0)}{d^2k\, dy} \tag{3.1}$$

where $d\sigma^{q\bar{q}A}(x_1, x_0)/d^2k\, dy$ is the gluon production cross section for the scattering of a colour dipole with quark coordinate x_1 and antiquark coordinate x_0 on the target, and $\psi^{\gamma^* \to q\bar{q}}(x_{01}, z)$ is the well-known [20] wave function of the splitting of the virtual photon in DIS into $q\bar{q}$ pair with of a transverse size $x_{10} = x_1 - x_0$ and a fraction z of the longitudinal momentum of the photon carried by the quark.

We want to point out that we limit our discussion to a case where the produced gluon is the hardest gluon emitted in $q\bar{q}$ system.

We start with selecting only those diagrams from Fig. 4, which have a real gluon emission (the soft gluon appears at the cut at $\tau = \infty$). It is easy to see that we are left with A, B (B^*) and D. In the inclusive cross section the transverse momentum k of the soft gluon is kept fixed and thus transverse coordinates of the produced gluon are different in the amplitude (x_2) and the conjugate amplitude ($x_{2'}$). Before writing the expression for the inclusive cross section with one gluon production we define an object which will play a central role in our further derivations. The function $M(12|34)$ is defined as an unintegrated over the impact parameter cross section of the scattering of a dipole with coordinates of quark (antiquark) being x_1 (x_2) in the amplitude and x_3 (x_4) in the conjugate amplitude. One should keep in mind that the cross section $M(12|34)$ is a function of rapidity though it is not reflected in our notation. The explicit expression for $M(12|34) = M_0(12|34)$ in the case of interaction with a nucleus without evolution is given in Appendix B. In fact, we have three of them, for each of the diagrams A, B (B^*) and D in Fig. 4. In Section 4 we show that all three functions are described by the same evolution equation and obey a generalized form of the optical theorem for the case of the dipole having different sizes in the amplitude and the conjugate amplitude.

[1] For simplicity, we omit the argument $Y = log(1/x_{Bjorken})$ where $x_{Bjorken}$ is the fraction of energy carried by the dipole.

We are ready to write the expression for the inclusive cross section in terms of M^A, M^B and M^D as follows [2]

$$\frac{d\sigma^{q\bar{q}A\to GX}(x_1,x_0)}{d^2kdy} = \frac{\bar{\alpha_s}}{2\pi}\frac{1}{(2\pi)^2}\int d^2x_2 d^2x_{2'} e^{-ik(x_2-x_{2'})}\left\{\left(\frac{x_{12}}{x_{12}^2}-\frac{x_{02}}{x_{02}^2}\right)\left(\frac{x_{12'}}{x_{12'}^2}-\frac{x_{02'}}{x_{02'}^2}\right)\left(M_0(12|12')+M_0(20|2'0)\right.\right. \tag{3.2}$$

$$\left.\left.+M_0(12|12')M_0(20|2'0)-M_0(12|12')\left\{N_0(20)+N_0(2'0)\right\}-M_0(20|2'0)\left\{N_0(12)+N_0(12')\right\}+N_0(20)N_0(12')+N_0(12)N_0(20')\right) \tag{3.3}$$

$$-\left(\frac{x_{12}}{x_{12}^2}-\frac{x_{02}}{x_{02}^2}\right)\left(0-\frac{x_{02'}}{x_{02'}^2}\right)\left\{M_0(12|10)\left(1-N_0(20)\right)+N_0(20)N_0(10)\right\} \tag{3.4}$$

$$-\left(\frac{x_{12}}{x_{12}^2}-\frac{x_{02}}{x_{02}^2}\right)\left(\frac{x_{12'}}{x_{12'}^2}-0\right)\left\{M_0(20|10)\left(1-N_0(12)\right)+N_0(10)N_0(12)\right\}$$

$$-\left(0-\frac{x_{02}}{x_{02}^2}\right)\left(\frac{x_{12'}}{x_{12'}^2}-\frac{x_{02'}}{x_{02'}^2}\right)\left\{M_0(10|12')\left(1-N_0(2'0)\right)+N_0(10)N_0(2'0)\right\} \tag{3.5}$$

$$-\left(\frac{x_{12}}{x_{12}^2}-0\right)\left(\frac{x_{12'}}{x_{12'}^2}-\frac{x_{02'}}{x_{02'}^2}\right)\left\{M_0(10|2'0)\left(1-N_0(12')\right)+N_0(10)N_0(12')\right\}$$

$$\left.+\left(\frac{x_{12}}{x_{12}^2}\frac{x_{12'}}{x_{12'}^2}+\frac{x_{02}}{x_{02}^2}\frac{x_{02'}}{x_{02'}^2}\right)M_0(10|10)-\left(\frac{x_{12}}{x_{12}^2}\frac{x_{02'}}{x_{02'}^2}+\frac{x_{02}}{x_{02}^2}\frac{x_{12'}}{x_{12'}^2}\right)N_0^2(10)\right\} \tag{3.6}$$

where N_0 is the initial condition of BK equation and $M_0(ik|il)$ is given in Appendix B.

In Eq. (3.2) we account for a separate rescattering of dipoles "12" ("12′") and "20" ("2′0") coming from diagram A.

In Eq. (3.3) we include the contributions where both of the dipoles are rescattered at the same time in diagram A. The first term describes the case where the two dipoles are rescattered both elastically and inelastically. The second and the third terms represent both elastic and inelastic rescattering of one dipole and only elastic (either amplitude or conjugate amplitude) rescattering of the other dipole. The fourth and fifth terms describe only elastic rescattering of the two dipoles. One should note that terms $N_0(20)N_0(12')+N_0(12)N_0(20')$ are not included into $M_0(12|12')M_0(20|2'0)$ since the elastic part of the cross section $M_0(12|12')$ by the definition starts with the lowest order of $N_0(12)N_0(12')$ (there are no disconnected diagrams), and thus the terms $N_0(20)N_0(12')+N_0(12)N_0(20')$ should be added separately.

In Eq. (3.4) we have contributions from diagram $B(B^*)$ which are not symmetrical in the Kernel. Namely, some diagrams are prohibited by the definition of the cross section $M_0(12|10)$. As a simple example, we try to include contributions which do not enter Eq. (3.4). We consider $\frac{x_{12}}{x_{12}^2}\frac{x_{12'}}{x_{12'}^2}M_0(12|10)$ as shown in Fig. 5. It is immediately clear that $M_0(12|10)$ cannot multiply such a dipole splitting, since a dipole "12" ("10") is not present at the interaction time $\tau=0$ in the conjugate amplitude with such a dipole splitting $\frac{x_{12}}{x_{12}^2}\frac{x_{12'}}{x_{12'}^2}$. In other words, the dipole formed by the lower quark loop scatters only elastically.

The first term in Eq. (3.4) includes elastic and inelastic rescattering of only one dipole, and also elastic rescattering of the other dipole. The term $N_0(20)N_0(10)$ corresponds to the elastic scattering of the dipole "20" in the amplitude and the elastic scattering of the dipole "10" in the conjugate amplitude, as it was mentioned before this term is not present in $M(20|10)N(20)$ by the definition of $M(20|10)$ due to the absence of the disconnected diagrams. Same for all other terms in Eq. (3.4) and Eq. (3.5).

[2] In Eq. (3.2) and everywhere in this paper we use notation $k\,x$ instead of $\vec{k}_\perp\cdot\vec{x}_\perp$. We hope that this will not cause difficulty in understanding.

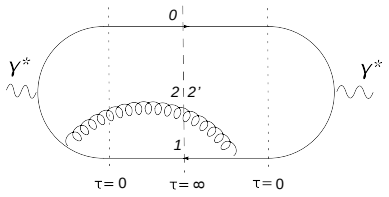

Figure 5: An example of a diagram that leads to asymmetric Kernels in Eq. (3.4) and Eq. (3.5).

Finally, in Eq. (3.6) we account for the contribution from diagram D, where we have both elastic and inelastic scatterings of the initial dipole "10". This can be easily understood from all D-type diagrams, where the measured gluon is emitted from quark and/or antiquark after the interaction time $\tau = 0$. In the case of "crossed" dipole splittings $\frac{x_{12}}{x_{12}^2}\frac{x_{02'}}{x_{02'}^2}$ etc. the inelastic rescattering is suppressed in large N_c, that is the reason why the last term in Eq. (3.6) has $N_0^2(10)$ instead of $M(10|10)$(which also includes the inelastic part).

As the last step in our derivation we have to substitute the expressions for the total cross section M_0 and the elastic amplitude N_0 by their eikonal formulae which are found in Appendix B. After some tedious, but straightforward algebra we obtain

$$\frac{d\sigma^{q\bar{q}A\to GX}(x_1,x_0)}{d^2k\,dy} = \frac{\bar{\alpha}_s}{2\pi}\frac{1}{(2\pi)^2}\int d^2x_2 d^2x_{2'} e^{-ik(x_2-x_{2'})}\left\{\frac{x_{02}}{x_{02}^2}\frac{x_{02'}}{x_{02'}^2}\left(1+e^{-2x_{22'}^2Q_s^2/4}-e^{-2x_{20}^2Q_s^2/4}-e^{-2x_{2'0}^2Q_s^2/4}\right)\right. \tag{3.7}$$

$$-\frac{x_{12}}{x_{12}^2}\frac{x_{02'}}{x_{02'}^2}\left(e^{-2x_{10}^2Q_s^2/4}+e^{-2x_{22'}^2Q_s^2/4}-e^{-2x_{12'}^2Q_s^2/4}-e^{-2x_{20}^2Q_s^2/4}\right) \tag{3.8}$$

$$-\frac{x_{02}}{x_{02}^2}\frac{x_{12'}}{x_{12'}^2}\left(e^{-2x_{10}^2Q_s^2/4}+e^{-2x_{22'}^2Q_s^2/4}-e^{-2x_{02'}^2Q_s^2/4}-e^{-2x_{21}^2Q_s^2/4}\right) \tag{3.9}$$

$$\left.+\frac{x_{12}}{x_{12}^2}\frac{x_{12'}}{x_{12'}^2}\left(1+e^{-2x_{22'}^2Q_s^2/4}-e^{-2x_{12}^2Q_s^2/4}-e^{-2x_{12'}^2Q_s^2/4}\right)\right\} \tag{3.10}$$

which is the result obtained by Kovchegov in [8]. At first sight, there is a difference of the factor of 2 in the exponentials, which comes from effective double interaction of the same dipole. At this point we have to clarify this coefficient in powers of the exponentials in Eqs. (3.7)-(3.10). We found some confusion in the literature regarding this coefficient, it varies from 1/4 to 1/2 depending on the author and even sometimes for the same author. This confusion stems from the definition of the saturation scale for a quark or a gluon which differs by a factor of 2. We use the quark saturation scale throughout the paper having a coefficient 1/2 in the exponentials of Eqs. (3.7)-(3.10). The physical meaning of this is explained as follows.

The important feature of the expression for the inclusive single gluon production Eqs. (3.7)-(3.10) is that interaction happens only to the emitted soft gluon and a quark(antiquark) from which it was emitted. The interaction of a quark (antiquark) which does not emit the soft gluon cancels and can be schematically explained as follows. In terms of the amplitude, diagrams A, $B(B^*)$ and D in Fig. 4 have only two possibilities for the real soft gluon: to emitted either before or after the interaction time $\tau = 0$ as shown in Fig. 6.

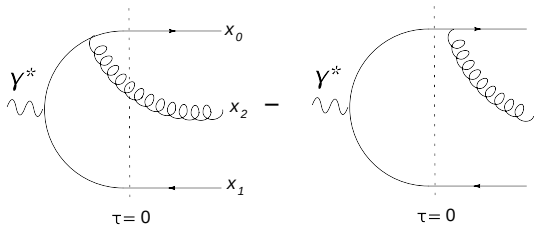

Figure 6: This illustrates the fact that in the low energy limit the interaction occurs only with the produced gluon and a quark (antiquark) from which it was emitted. The cancellation leads to effective interaction twice with the same (upper) dipole.

The emission after $\tau = 0$ has a minus sign w.r.t the emission before $\tau = 0$, which can be easily checked by considering light-cone energy denominators (see for example [14, 8, 9, 10] and also Appendix A). For simplicity, consider one t-channel gluon interaction with the target for each dipole (12) and (20) formed by the soft gluon emission. In this case we have two contributions in the transverse coordinate space for the lower dipole

$$\int \frac{d^2l}{l^2} \left\{ \left(e^{-ilx_1} - e^{-ilx_0}\right) - \left(e^{-ilx_1} - e^{-ilx_2}\right) \right\} = \int \frac{d^2l}{l^2} \left(e^{-ilx_2} - e^{-ilx_0}\right) \tag{3.11}$$

the upper dipole has only one contribution

$$\int \frac{d^2l}{l^2} \left(e^{-ilx_2} - e^{-ilx_0}\right) \tag{3.12}$$

From Eq. (3.11) and Eq. (3.12) one can see that the two contributions for the lower dipole effectively sum into interaction with the upper dipole. It should be mentioned that one cannot sum Eq. (3.11) and Eq. (3.12) in the amplitude since they have different colour matrices, but after multiplication by conjugate amplitude one obtains the same colour factor which results into a factor of 2 in the exponentials in Eqs. (3.7)-(3.10) and looks like a dipole interacts twice with the target (or two dipoles of the same size interact once). In the BK equation (written for total cross section) we do not observe this, since the second diagram in Fig. 6 cancels with corresponding virtual gluon emission. This *ad hoc* explanation is by no means an exhaustive one, but rather a simple argument why one should expect only the soft gluon and the quark (antiquark) from which it was emitted to interact with the target. A rigorous calculation shows the same result, provided we assign to the interaction with target the same expression before and after the gluon emission. Here we demonstrated how this happens in the case of the eikonal interaction at low energy with no evolution included. In the next Section we show that proper inclusion of the non-linear evolution effects does not change this general feature of the single inclusive cross section that the "spectator quark" never interacts with the target in the course of the evolution and thus all the interaction can be expressed in terms of the adjoint amplitude $N_G(x) = 2N(x) - N^2(x)$ as was suggested by Kovchegov and Tuchin in Ref. [9].

4. Inclusive gluon production with evolution

In this section we want to include the evolution into the expression for the single gluon inclusive cross section found in Section 3. It was suggested in Ref. [9] that each exponential in Eqs. (3.7)-(3.10) is to be replaced with a function $1 - N_G$, where N_G is the elastic scattering amplitude of an adjoint ("gluonic") dipole given by $N_G(22') = 2N(22') - N^2(22')$ with $N(22')$ being a solution for the BK equation.This substitution is based on the classical

expression where only the produced gluon and a quark(antiquark) from which it was emitted do interact with the target and thus in the course of the evolution one can safely ignore the spectator quark (antiquark). Kovchegov and Tuchin [9] analyzed the next step of the evolution in the rapidity where an extra softer gluon is emitted and found that this form also holds to this order. This way the authors generalized the result to any order of the softer gluon emissions. In this Section we use the expression for the single inclusive cross section Refs. (3.2-3.6) supplemented by the evolution equation for the function $M(ij|ik)$ to show explicitly the validity of the adjoint("gluonic") dipole structure at any order of the evolution.

We start with deriving the evolution equation for the function $M(ij|ik)$, which has the meaning of the total cross section for $j = k$. It should be emphasized that $M(ij|ik)$ is also a function of the rapidity though it is not indicated in our notation. We are interested in the evolution in rapidity where only softer gluons are emitted, the emission of the harder gluons can be easily included through the dipole density as it was shown by Kovchegov and Tuchin [9], and thus is not relevant for our discussion. We want to remind that we are interested only in the situation where the measured gluon is the hardest gluon in the system. In our derivation we help with a set of the simple mnemonic rules, as follows,

- the gluon is represented by a double quark line in the large N_C limit, the triple gluon vertex can be effectively written as an emission of the softer gluon from the quark and antiquark components of the harder gluon. The emission from the antiquark component of the harder gluon has a relative minus sign w.r.t. the emission from the quark component. For more details, see Ref. [14];
- the virtual emission (diagrams R,C, E and F in Fig. 4) has relative minus sign w.r.t. to the real emissions (diagrams A, B and D in Fig. 4). In addition to this, the diagrams where the virtual gluon is not present at the interaction time $\tau = 0$ has a factor of $1/2$ due to light cone time ordered integration. For more details, see Ref. [14];
- the softer gluon can be emitted only after the harder gluon before the interaction time $\tau = 0$, and only before the harder gluon after the interaction time. In the case where one of the gluons is emitted before $\tau = 0$ and the other one after $\tau = 0$, the light cone time ordering is arbitrary, irrespectively whether the soft or the hard gluon was emitted before $\tau = 0$. These light cone time ordering rules where derived by Jalilian-Marian and Kovchegov [10] using light cone energy denominators.

We would like to comment more on the last light cone time ordering rule. This rule implies that a softer gluon can be emitted only from a dipole which was present at $\tau = 0$, this means the all the information about further evolution can be encoded in the function $M(ij|ik)$ through specifying the coordinates of the dipoles present at $\tau = 0$ in the amplitude and conjugate amplitude (and, of course, the energy variable not reflected in our notation). In the more general case, where the rapidity separation between two adjacent emitted gluons is not large (multi Regge kinematics does not hold) one has also to specify the dipoles present at $\tau = \infty$.

We are ready to write the evolution equation for the function $M(12|12')$, which has a meaning of the total scattering cross section for a dipole having quark at x_1 and antiquark at x_2 in the amplitude, as well as, quark at x_1 and antiquark at x_2' in the complex conjugate amplitude. We analyze the emission of a softer gluon with transverse coordinate x_3 in the dipole "12"("12′"). Working in the large N_C limit we represent the gluons by double quark-antiquark line and show them disconnected from other lines reflecting all possible couplings to quark or antiquark line in accordance with the notation used in [9]. In analogy with Fig. 4 consider all possible emissions of gluon "3" in the dipole "12"("12′") depicted in Fig. 7 (diagram B^* and C^* are not shown, but must be included as well).

The evolution equation is found by accounting for all interaction possibilities of the system of the initial dipole with one extra softer gluon emission depicted in Fig. 7 (together with diagrams B^* and C^* not shown in Fig. 7).

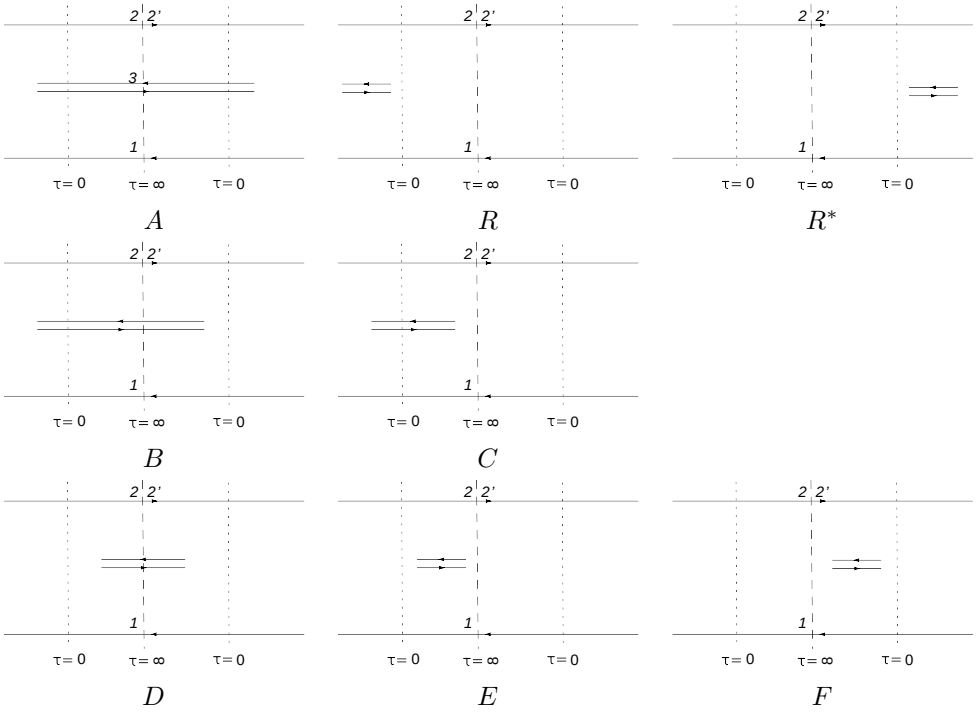

Figure 7: All possible emissions of the softer gluon "3" in the dipole "12"("12′"), diagrams B^* and C^* are not shown.

The corresponding evolution equation is given by

$$\frac{\partial M(12|12')}{\partial y} = \frac{\bar{\alpha}_s}{2\pi}\int d^2x_3 \left\{ -\frac{1}{2}\left(\frac{x_{13}}{x_{13}^2} - \frac{x_{23}}{x_{23}^2}\right)^2 M(12|12') - \frac{1}{2}\left(\frac{x_{13}}{x_{13}^2} - \frac{x_{2'3}}{x_{2'3}^2}\right)^2 M(12|12') \right. \tag{4.1}$$

$$+ \left(\frac{x_{13}}{x_{13}^2} - \frac{x_{23}}{x_{23}^2}\right)\left(\frac{x_{13}}{x_{13}^2} - \frac{x_{2'3}}{x_{2'3}^2}\right)\left(M(13|13) + M(32|32') + M(13|13)M(32|32')\right. \tag{4.2}$$

$$\left. -M(32|32')\left\{N(13) + N(13)\right\} - M(13|13)\left\{N(32) + N(32')\right\} + N(13)N(32') + N(32)N(13)\right) \tag{4.3}$$

$$\begin{aligned}
&- \left(\frac{x_{13}}{x_{13}^2} - \frac{x_{23}}{x_{23}^2}\right)\left(0 - \frac{x_{2'3}}{x_{2'3}^2}\right)\left[M(13|12')\left\{1 - N(32)\right\} + N(32)N(12')\right] \\
&- \left(\frac{x_{13}}{x_{13}^2} - \frac{x_{23}}{x_{23}^2}\right)\left(\frac{x_{13}}{x_{13}^2} - 0\right)\left[M(32|12')\left\{1 - N(13)\right\} + N(13)N(12')\right] \\
&- \left(0 - \frac{x_{23}}{x_{23}^2}\right)\left(\frac{x_{13}}{x_{13}^2} - \frac{x_{2'3}}{x_{2'3}^2}\right)\left[M(12|13)\left\{1 - N(32')\right\} + N(12)N(32')\right] \\
&- \left(\frac{x_{13}}{x_{13}^2} - 0\right)\left(\frac{x_{13}}{x_{13}^2} - \frac{x_{2'3}}{x_{2'3}^2}\right)\left[M(12|32')\left\{1 - N(13)\right\} + N(12)N(13)\right]
\end{aligned} \tag{4.4}$$

$$
\begin{aligned}
&+\left(\frac{x_{13}}{x_{13}^2}-\frac{x_{23}}{x_{23}^2}\right)\left(0-\frac{x_{23}}{x_{23}^2}\right)\left[M(13|12')\left\{1-N(32)\right\}+N(32)N(12')\right] \\
&+\left(\frac{x_{13}}{x_{13}^2}-\frac{x_{23}}{x_{23}^2}\right)\left(\frac{x_{13}}{x_{13}^2}-0\right)\left[M(32|12')\left\{1-N(13)\right\}+N(13)N(12')\right] \\
&+\left(0-\frac{x_{2'3}}{x_{2'3}^2}\right)\left(\frac{x_{13}}{x_{13}^2}-\frac{x_{2'3}}{x_{2'3}^2}\right)\left[M(12|13)\left\{1-N(32')\right\}+N(12)N(32')\right] \\
&+\left(\frac{x_{13}}{x_{13}^2}-0\right)\left(\frac{x_{13}}{x_{13}^2}-\frac{x_{2'3}}{x_{2'3}^2}\right)\left[M(12|32')\left\{1-N(13)\right\}+N(12)N(13)\right]
\end{aligned}
\tag{4.5}
$$

$$
\begin{aligned}
&+\left(\frac{x_{23}}{x_{23}^2}\frac{x_{2'3}}{x_{2'3}^2}+\frac{x_{13}}{x_{13}^2}\frac{x_{13}}{x_{13}^2}\right)M(12|12')-\left(\frac{x_{23}}{x_{23}^2}\frac{x_{13}}{x_{13}^2}+\frac{x_{13}}{x_{13}^2}\frac{x_{2'3}}{x_{2'3}^2}\right)N(12)N(12') \\
&-\frac{1}{2}\left(\frac{x_{23}}{x_{23}^2}\frac{x_{23}}{x_{23}^2}+\frac{x_{13}}{x_{13}^2}\frac{x_{13}}{x_{13}^2}\right)M(12|12')+\frac{1}{2}\left(\frac{x_{23}}{x_{23}^2}\frac{x_{13}}{x_{13}^2}+\frac{x_{13}}{x_{13}^2}\frac{x_{23}}{x_{23}^2}\right)N(12)N(12') \\
&-\frac{1}{2}\left(\frac{x_{2'3}}{x_{2'3}^2}\frac{x_{2'3}}{x_{2'3}^2}+\frac{x_{13}}{x_{13}^2}\frac{x_{13}}{x_{13}^2}\right)M(12|12')+\frac{1}{2}\left(\frac{x_{2'3}}{x_{2'3}^2}\frac{x_{13}}{x_{13}^2}+\frac{x_{13}}{x_{13}^2}\frac{x_{2'3}}{x_{2'3}^2}\right)N(12)N(12')\Bigg\}
\end{aligned}
\tag{4.6}
$$

with N being a solution to the BK equation.

Each contribution is explained as follows

- The two terms on the r.h.s of Eq. (4.1) come from the diagrams R and R^* in Fig. 7 and represent the reggeization. Their Kernels are different and correspond to emission and absorption of the softer gluon "3" in the amplitude for diagram R, and the emission and absorption of the softer gluon "3" in the conjugate amplitude for diagram R^*. A factor of $\frac{1}{2}$ appears due to time ordered integral in the light-cone time (for more details see Appendix of Ref. [14]).

- Terms in Eq. (4.2) stand for the interaction of each dipole with the target as shown in diagram A. Their Kernel corresponds to the emission of the softer gluon "3" in the amplitude and its absorption in the conjugate amplitude. The last non-linear term in Eq. (4.2) describes the situation where the two dipoles scatter both elastically and inelastically off the target simultaneously.

- For all the terms in Eq. (4.3) we have we same Kernel as for terms in Eq. (4.2) since emission and absorption of the softer gluon is the same. The first and the second terms reflect the situation where one of the dipoles rescatter both elastically and inelastically, and the other one rescatters only elastically in either amplitude or conjugate amplitude. These contributions are not present in $M(13|13)M(32|32')$ since M by the definition includes inelastic part and elastic scattering *both* in the amplitude and the scattering amplitude (in other words, only N^2 and not N). The last term corresponds to the situation where the two dipole rescatter elastically, one in the amplitude and another in conjugate amplitude, and *vice versa*.

- The same analysis implies in Eq. (4.4) requiring the proper counting of all interaction patterns in diagrams B (first two lines) and B^* (last two lines) in Fig. 7. The zero term in the asymmetric Kernel used here stands for situation where the dipole "13"("12'") is not present by time $\tau = 0$ in the conjugate amplitude and thus is omitted as was explained in more details in Section 3. The last two lines of Eq. (4.4) correspond to the diagram B^*, which is the conjugate of diagram B in Fig. 7

- In Eq. (4.5) we account for diagram C(first two lines) and diagram C^*(last two lines) using the same arguments as for Eq. (4.4). The only difference between the corresponding lines of Eq. (4.4) and Eq. (4.5) is the Kernel

of the dipole splitting, namely, in Eq. (4.4) the soft gluon 3 is present at $\tau = \infty$, and in Eq. (4.5) is not. If the initial dipole "12"("12′") has the same coordinates in the amplitude and the conjugate amplitude then the corresponding lines of Eq. (4.4) and Eq. (4.5) are subject to their mutual cancellation (real-virtual cancellations) and was shown by Chen and Muller [14].

- In Eq. (4.6) we write the contributions of diagrams D, E and F in Fig. 7. Here one should note that in the crossed dipole splittings (i.e. $\frac{x_{13}}{x_{13}^2}\frac{x_{23}}{x_{23}^2}$ etc.) the inelastic interaction are suppressed in the large N_C limit, this is the origin of the terms $N(12)N(12')$.

The evolution equation should be supplemented by the initial condition M_0 given by Eq. (B-12)

$$M_0(12|12') \;=\; 1 + e^{-x_{22'}^2 Q_s^2/4} - e^{-x_{12}^2 Q_s^2/4} - e^{-x_{12'}^2 Q_s^2/4} \tag{4.7}$$

One can easily see that due to the equality of the quark coordinate x_1 in the amplitude and the conjugate amplitude, some terms cancel each other in the evolution equation Eqs. (4.1)-(4.5). For example, the second line in Eq. (4.4) cancels the second line in Eq. (4.5). Some further cancellations happen because of the optical theorem. The optical theorem states that the total cross section equals twice the imaginary part of the scattering amplitude $M(12|12) = 2N(12)$. This implies that the last term in Eq. (4.2) cancels the first term in Eq. (4.3).

The simplified form of the evolution equation Eqs. (4.1)-(4.5) is given by

$$\frac{\partial M(12|12')}{\partial y} = \frac{\bar{\alpha}_s}{2\pi}\int d^2x_3 \left\{ -\frac{1}{2}\left(\frac{x_{13}}{x_{13}^2} - \frac{x_{23}}{x_{23}^2}\right)^2 M(12|12') - \frac{1}{2}\left(\frac{x_{13}}{x_{13}^2} - \frac{x_{2'3}}{x_{2'3}^2}\right)^2 M(12|12') \right. \tag{4.8}$$

$$+ \left(\frac{x_{13}}{x_{13}^2} - \frac{x_{23}}{x_{23}^2}\right)\left(\frac{x_{13}}{x_{13}^2} - \frac{x_{2'3}}{x_{2'3}^2}\right)\{2N(13) + M(32|32') - N(13)N(32') - N(32)N(13)\} \tag{4.9}$$

$$- \left(\frac{x_{13}}{x_{13}^2} - \frac{x_{23}}{x_{23}^2}\right)\left(\frac{x_{23}}{x_{23}^2} - \frac{x_{2'3}}{x_{2'3}^2}\right)[M(13|12')\{1 - N(32)\} + N(32)N(12')] \tag{4.10}$$

$$- \left(\frac{x_{2'3}}{x_{2'3}^2} - \frac{x_{23}}{x_{23}^2}\right)\left(\frac{x_{13}}{x_{13}^2} - \frac{x_{2'3}}{x_{2'3}^2}\right)[M(12|13)\{1 - N(32')\} + N(12)N(32')]$$

$$\left. - \frac{1}{2}\left(\frac{x_{23}}{x_{23}^2} - \frac{x_{2'3}}{x_{2'3}^2}\right)^2 M(12|12') \right\} \tag{4.11}$$

To see the consistency with the previous studies one can take $2 = 2'$ and use the optical theorem to recover the BK equation. In this case Eq. (4.10) and Eq. (4.11) vanish, Kernels in Eq. (4.8) and Eq. (4.9) become equal and we end up with with the evolution equation

$$\frac{\partial(2N(12))}{\partial y} = \frac{\bar{\alpha}_s}{2\pi}\int d^2x_3 \left(\frac{x_{13}}{x_{13}^2} - \frac{x_{23}}{x_{23}^2}\right)^2 \{2N(13) + 2N(32) - 2N(13)N(32)\} \tag{4.12}$$

with the initial condition directly obtained from (see Eq. (B-12))

$$M_0(12|12') = 1 + e^{-x_{22'}^2 Q_{so}^2/4} - e^{-x_{12}^2 Q_{so}^2/4} - e^{-x_{12'}^2 Q_{so}^2/4} \tag{4.13}$$

for $2 = 2'$ as follows $M_0(12|12) = 2\left(1 - e^{-x_{12}^2 Q_{so}^2/4}\right) = 2N_0(12)$. Thus the evolution equation is the BK equation with the correct initial condition.

Next step is to study general properties and to find a solution to the evolution equation Eqs. (4.8)-(4.11). At this point we make a digression and go back to the classical expression for the single inclusive production cross section Eqs. (3.2)-(3.6). As one can easily see, the cancellation of the emissions with the "spectator" quark (antiquark) found by Kovchegov [8] in the form of Eqs. (3.7)-(3.10) can happen only if $M_0(12|10) = N_0(12) + N_0(10) - N_0(20)$, where in the last term $20 = (10) - (12)$. The initial condition Eq. (4.13) indeed satisfies this condition. If one wants to include the evolution effects, the function M_0 in Eqs. (3.2)-(3.6) should be replaced by the solution to the evolution equation Eqs. (4.8)-(4.11) with the initial condition given by Eq. (4.13). This suggests that $M(12|12')$ should also have this property to result into the cancellation of the emissions and the interactions with the "spectator" quark (antiquark) line. The straightforward substitution of

$$M(12|12') = N(12) + N(12') - N(22') \tag{4.14}$$

into Eqs. (4.8)-(4.11) reveals

$$\frac{\partial(N(12) + N(12') - N(22'))}{\partial y} = \frac{\bar{\alpha_s}}{2\pi} \int d^2x_3 \left\{ -\frac{1}{2} \left(\left(\frac{x_{13}}{x_{13}^2} - \frac{x_{23}}{x_{23}^2} \right)^2 + \left(\frac{x_{13}}{x_{13}^2} - \frac{x_{2'3}}{x_{2'3}^2} \right)^2 \right) (N(12) + N(12') - N(22')) \right. \tag{4.15}$$

$$+ \left(\frac{x_{13}}{x_{13}^2} - \frac{x_{23}}{x_{23}^2} \right) \left(\frac{x_{13}}{x_{13}^2} - \frac{x_{2'3}}{x_{2'3}^2} \right) \left\{ 2N(13) + (N(32) + N(32') - N(22')) - N(13)N(32') - N(32)N(13) \right\} \tag{4.16}$$

$$- \left(\frac{x_{13}}{x_{13}^2} - \frac{x_{23}}{x_{23}^2} \right) \left(\frac{x_{23}}{x_{23}^2} - \frac{x_{2'3}}{x_{2'3}^2} \right) \left[\left(N(13) + N(12') - N(32') \right) \left\{ 1 - N(32) \right\} + N(32)N(12') \right] \tag{4.17}$$

$$- \left(\frac{x_{2'3}}{x_{2'3}^2} - \frac{x_{23}}{x_{23}^2} \right) \left(\frac{x_{13}}{x_{13}^2} - \frac{x_{2'3}}{x_{2'3}^2} \right) \left[\left(N(12) + N(13) - N(32) \right) \left\{ 1 - N(32') \right\} + N(12)N(32') \right]$$

$$\left. - \frac{1}{2} \left(\frac{x_{23}}{x_{23}^2} - \frac{x_{2'3}}{x_{2'3}^2} \right)^2 \left(N(12) + N(12') - N(22') \right) \right\} \tag{4.18}$$

which is just a linear combination of three BK equations for initial dipoles with coordinates 12, $12'$ and $22'$

$$\frac{\partial(N(12) + N(12') - N(22'))}{\partial y} = \frac{\bar{\alpha_s}}{2\pi} \int d^2x_3 \left\{ \left(\frac{x_{13}}{x_{13}^2} - \frac{x_{23}}{x_{23}^2} \right)^2 \left\{ N(13) + N(32) - N(12) - N(13)N(32) \right\} \right. \tag{4.19}$$

$$+ \left(\frac{x_{13}}{x_{13}^2} - \frac{x_{2'3}}{x_{2'3}^2} \right)^2 \left\{ N(13) + N(32') - N(12') - N(13)N(32') \right\} \tag{4.20}$$

$$\left. - \left(\frac{x_{23}}{x_{23}^2} - \frac{x_{2'3}}{x_{2'3}^2} \right)^2 \left\{ N(32) + N(32') - N(22') - N(32)N(32') \right\} \right\} \tag{4.21}$$

This way we show explicitly that indeed the cancellations claimed by Kovchegov and Tuchin [9] hold to any order of evolution, allowing for the simple description of the single inclusive cross section in terms of the combination $2N(x) - N^2(x)$, which can be interpreted as the scattering amplitude $N_G(x)$ of an adjoint("gluonic") dipole of size x.

In the next Section we examine the Abramovsky-Gribov-Kancheli cutting rules in pQCD using the formalism we developed for the calculation of the single production cross section.

5. Abramovsky-Gribov-Kancheli cutting rules

More than 30 years ago Abramovsky,Gribov and Kancheli [5] analyzed the relative contributions of processes with different multiplicity of the produced particles to the total cross section of the multiple Pomeron exchange in the framework of the Reggeon Field Theory. They found that the contributions of different unitarity cuts, corresponding to different particle multiplicities are proportional to each other (AGK cutting rules), and their relative coefficients lead to some peculiar cancellations, called AGK cancellations for the single jet production. The most interesting case is the two Pomeron exchange, where the AGK cancellation can be explained as follows. The total cross section is given by the sum of all possible unitarity cuts. The Pomeron is non-local object, so it can be also cut enlarging the number of cut possibilities. This way one obtains two distinct objects - cut and uncut Pomerons, which are to be treated separately as far as multiplicity is concerned. The simplest example for this is the two Pomeron exchange depicted in Fig. 8. As one can see we have here three different processes: *a*) *double cut*, where the two Pomerons are

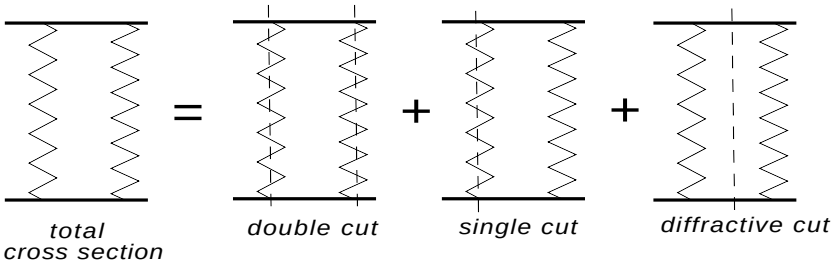

Figure 8: The total cross section of two Pomeron exchange in terms of contributions from different s-channel unitarity cuts. The double cut diagram describes the process with the multiplicity two times larger the multiplicity for one Pomeron exchange (see Fig. 1), the single cut diagrams leads to a process with the same multiplicity as one Pomeron exchange (see Fig. 1) and the diffractive cut diagram gives the expression for a diffractive production with small multiplicity.

cut. This brings two times multiplicity of one cut Pomeron; *b*) *single cut*, one Pomeron appears cut and the other one is uncut. The multiplicity of this process equals the multiplicity of one cut Pomeron; *c*) *diffractive cut*, here two Pomerons are uncut and no particles are produced. The multiplicity of this process is very small. The relative weights of three processes are calculated as follows. There only one possibility to cut two Pomerons at the same time, each cut Pomeron is twice the uncut Pomeron exchange (due to the unitarity condition $I\!P = 2P$), thus we obtain $4P^2$. For the single cut we have two possibilities: to cut one of two Pomerons, this must be multiplied by the a factor of 2 for putting the uncut Pomeron either in the amplitude or the conjugate amplitude. The resulting combinatorial coefficient of 4 is to be multiplied by a factor 2 for the normalization of the cut Pomeron ($I\!P = 2P$) as well as a minus sign originating from the fact that uncut Pomeron is the imaginary part of the scattering amplitude. Summarizing all this, one gets $-8P^2$ from the single cut. Finally, in the diffractive cut the combinatorial coefficient is 2 for interchanging the two Pomerons in the amplitude and the conjugate amplitude. All three cuts add up to $4P^2 - 8P^2 + 2P^2 = -2P^2 = \sigma_{tot}^{(2)}$, as expected.

This set of the AGK coefficients results into cancellation of the single jet production as shown in Fig. 9

The jet can be produced from either of two cut Pomerons in the double cut, and only from the cut Pomeron in the single cut, resulting into the cancellation of the single jet production in the two Pomeron exchange. In this Section we treat the contributions from the different unitarity cuts in pQCD in the framework of the color dipole model. The goal of this study is to see how the AGK cancellations happen in the color dipole model and check in this way the validity of the AGK cutting rules in pQCD.

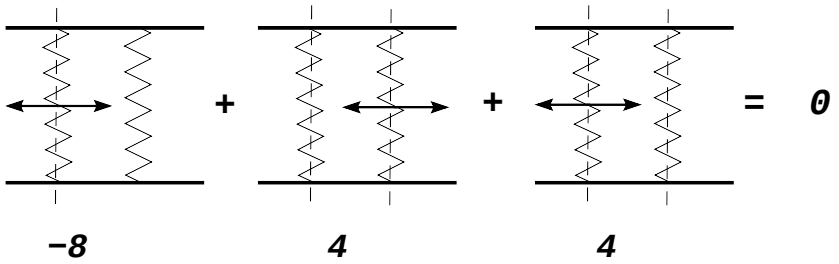

Figure 9: The cancellation of the single jet production for two Pomeron exchange.

In the original derivation of the AGK cutting rules [5] some basic assumptions were made, namely,

- Pomeron is a proper asymptotics in the high energy scattering;
- there are no "half-cut" Pomerons, the contributions where a Pomeron is not cut entirely are suppressed exponentially in the invariant mass;
- there is no contribution to the multiplicity from the cut of the vertices;
- all the vertices for various cuts are the same and real.

In the AGK paper [5] all these assumptions have been proved in the superconverged field theories, since they guarantee that all scattering amplitudes decrease in the region of large masses. As has been shown in Ref. [1] in the leading $log(1/x)$ approximation of perturbative QCD, the amplitudes fall in the region of high mass fast enough to hope that AGK cutting rules are correct. However, in addition to the assumptions that discussed above, it was also assumed in Ref. [5] that the multiparticle production is described by the same set of diagram as the total cross section. This assumption was doubtful even in a superconverged theory, since it was found that there is an example of the diagrams that does not contribute to the total cross section, but could lead to the multiparticle production (the AFS-type of diagrams [26]). Therefore, our main goal is to find what types of diagrams indeed contribute to the total and inelastic cross sections and to calculate the relation between different production processes.

Our strategy is as follows. We use the formalism developed in the previous Sections for deriving cutting rules in pQCD, then we analyze the single inclusive production of the two Pomeron exchange and check how the emission of the gluon changes the cutting rules. The process we discuss is the dipole scattering on the target via two Pomeron exchange: *a*) two Pomerons couple to the dipole; *b*) one Pomeron couples to the dipole and then splits into two Pomerons. The first case trivially satisfies AGK cutting rules and thus is of no interest. We focus on the second case depicted in Fig. 10. At this stage we do not consider any gluon production and want to analyze only the two Pomeron exchange in terms of the contributions of different cuts.

Schematically, this process can be written as

$$\sigma = \int P(Y - Y_0) \otimes \Gamma_{3P} \otimes P^2(Y_0 - 0) \tag{5.1}$$

where $P(Y - Y_0)$ is the Pomeron amplitude and Γ_{3P} is the triple Pomeron vertex. In the case of the virtual photon scattering on the target this is given by

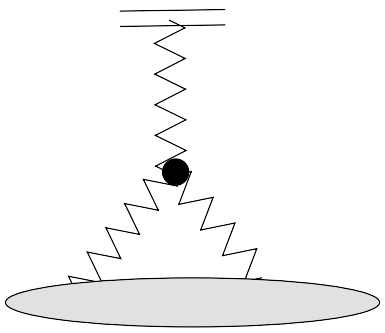

Figure 10: We check the validity the AGK cutting rules for the process of one to two Pomeron splitting.

$$\sigma = \int d^2x_{\tilde{1}} d^2x_{\tilde{0}} dz\ d^2x_1 d^2x_0\ |\psi^{\gamma^* \to q\bar{q}}(x_{\tilde{1}\tilde{0}}, \tilde{z})|^2 n(x_{\tilde{1}}, x_{\tilde{0}}|x_1, x_0; Y - Y_0) \sigma_{2P}^{q\bar{q}}(x_1, x_0) \tag{5.2}$$

where $\psi^{\gamma^* \to q\bar{q}}(x_{\tilde{1}\tilde{0}}, \tilde{z})$ is the wave function of the virtual photon being split into $q\bar{q}$ pair, $n(x_{\tilde{1}}, x_{\tilde{0}}|x_1, x_0; Y - Y_0)$ is the dipole density, which is the solution to the linear evolution equation. The triple Pomeron vertex and the interaction with the target is encoded into $\sigma_{2P}^{q\bar{q}}(x_1, x_0)$. Using the formalism developed in the previous Sections we can readily write an expression for $\sigma_{2P}^{q\bar{q}}(x_1, x_0)$ as

$$\begin{aligned}
\sigma_{2P}^{q\bar{q}}(x_1, x_0) = \frac{\bar{\alpha}_s}{2\pi} \int_0^{Y_0} dy \int d^2x_2 \left(\frac{x_{12}}{x_{12}^2} - \frac{x_{02}}{x_{02}^2} \right)^2 \Big\{ M_{lin}(12|12) M_{lin}(20|20) + \frac{1}{2} \left(M_{lin}(12|12) \right)^2 \\
+ \frac{1}{2} \left(M_{lin}(20|20) \right)^2 - \frac{1}{2} \left(M_{lin}(10|10) \right)^2 - \{ M_{lin}(12|12) + M_{lin}(20|20) \} \{ 2N_{\text{BFKL}}(12) + 2N_{\text{BFKL}}(20) \} \\
+ M_{lin}(10|10) 2N_{\text{BFKL}}(10) + 2N_{\text{BFKL}}(12) N_{\text{BFKL}}(20) + \left(N_{\text{BFKL}}(12) \right)^2 + \left(N_{\text{BFKL}}(20) \right)^2 - \left(N_{\text{BFKL}}(10) \right)^2 \Big\}
\end{aligned} \tag{5.3}$$

where N_{BFKL} and M_{lin} are solutions to the BFKL equation and some linear evolution equation as explained below.

In Eq. (5.3) the triple Pomeron vertex is represented by the initial dipole "10" which splits into two new dipoles "12" and "02", each of them can interact with the target elastically by the BFKL amplitude N_{BFKL} and inelastically by the inelastic cross section M_{lin}. If the same dipole interacts twice inelastically we put a factor of $\frac{1}{2}$ for the identity of the interactions. We have to take into account all possible splittings of the initial dipole as shown in Fig. 7, since most of the splittings are canceled by the real-virtual cancellations and we are left with diagrams A, R and R^*. The inelastic cross section M_{lin} is the solution to the linear evolution equation, obtained from the non-linear evolution equation Eqs. (4.1)-(4.6) retaining only the its linear part. In the contrary to the the non-linear case we do not include multiple rescattering in the initial condition for M_{lin}, which now consists of only two t-channel gluon exchange. In this case the total cross section equals the inelastic cross section and M_{lin} is associated with a cut Pomeron. For the non-linear case, where the multiple rescattering is taken into account the solution to Eqs. (4.1)-(4.6) includes both cut and uncut Pomeron exchanges, which can be extracted by expanding the total cross section in terms of the Pomerons as we show below. As we have already mentioned the linear evolution equation for M_{lin} is readily obtained from Eqs. (4.1)-(4.6) neglecting the non-linear terms as

$$\frac{\partial M_{lin}(12|12')}{\partial y} = \frac{\bar{\alpha}_s}{2\pi} \int d^2x_3 \left\{ -\frac{1}{2} \left(\frac{x_{13}}{x_{13}^2} - \frac{x_{23}}{x_{23}^2} \right)^2 M_{lin}(12|12') - \frac{1}{2} \left(\frac{x_{13}}{x_{13}^2} - \frac{x_{2'3}}{x_{2'3}^2} \right)^2 M_{lin}(12|12') \right. \tag{5.4}$$

$$+\left(\frac{x_{13}}{x_{13}^2}-\frac{x_{23}}{x_{23}^2}\right)\left(\frac{x_{13}}{x_{13}^2}-\frac{x_{2'3}}{x_{2'3}^2}\right)\{M_{lin}(13|13)+M_{lin}(32|32')\} \tag{5.5}$$

$$\begin{aligned}
&-\left(\frac{x_{13}}{x_{13}^2}-\frac{x_{23}}{x_{23}^2}\right)\left(0-\frac{x_{2'3}}{x_{2'3}^2}\right)M_{lin}(13|12') \\
&-\left(\frac{x_{13}}{x_{13}^2}-\frac{x_{23}}{x_{23}^2}\right)\left(\frac{x_{13}}{x_{13}^2}-0\right)M_{lin}(32|12') \\
&-\left(0-\frac{x_{23}}{x_{23}^2}\right)\left(\frac{x_{13}}{x_{13}^2}-\frac{x_{2'3}}{x_{2'3}^2}\right)M_{lin}(12|13) \\
&-\left(\frac{x_{13}}{x_{13}^2}-0\right)\left(\frac{x_{13}}{x_{13}^2}-\frac{x_{2'3}}{x_{2'3}^2}\right)M_{lin}(12|32')
\end{aligned} \tag{5.6}$$

$$\begin{aligned}
&+\left(\frac{x_{13}}{x_{13}^2}-\frac{x_{23}}{x_{23}^2}\right)\left(0-\frac{x_{23}}{x_{23}^2}\right)M_{lin}(13|12') \\
&+\left(\frac{x_{13}}{x_{13}^2}-\frac{x_{23}}{x_{23}^2}\right)\left(\frac{x_{13}}{x_{13}^2}-0\right)M_{lin}(32|12') \\
&+\left(0-\frac{x_{2'3}}{x_{2'3}^2}\right)\left(\frac{x_{13}}{x_{13}^2}-\frac{x_{2'3}}{x_{2'3}^2}\right)M_{lin}(12|13) \\
&+\left(\frac{x_{13}}{x_{13}^2}-0\right)\left(\frac{x_{13}}{x_{13}^2}-\frac{x_{2'3}}{x_{2'3}^2}\right)M_{lin}(12|32')
\end{aligned} \tag{5.7}$$

$$\begin{aligned}
&+\left(\frac{x_{23}}{x_{23}^2}\frac{x_{2'3}}{x_{2'3}^2}+\frac{x_{13}}{x_{13}^2}\frac{x_{13}}{x_{13}^2}\right)M_{lin}(12|12') \\
&-\frac{1}{2}\left(\frac{x_{23}}{x_{23}^2}\frac{x_{23}}{x_{23}^2}+\frac{x_{13}}{x_{13}^2}\frac{x_{13}}{x_{13}^2}\right)M_{lin}(12|12') \\
&-\frac{1}{2}\left(\frac{x_{2'3}}{x_{2'3}^2}\frac{x_{2'3}}{x_{2'3}^2}+\frac{x_{13}}{x_{13}^2}\frac{x_{13}}{x_{13}^2}\right)M_{lin}(12|12')\Bigg\}
\end{aligned} \tag{5.8}$$

with the initial condition given by

$$M_{lin_0}(12|12')=\frac{\bar{\alpha}_s}{8\pi}\int d^2k\frac{(e^{-ikx_1}-e^{-ikx_2})(e^{ikx_1}-e^{ikx_{2'}})}{k^4}IF(k^2) \tag{5.9}$$

where $IF(k^2)$ is the impact factor of the target.

The terms on r.h.s of Eq. (5.4) are the contributions from the diagrams R and R^* in Fig. 7, Eq. (5.5) comes from diagram A, Eq. (5.6) account for diagrams B and B^*, Eq. (5.7) stands for diagrams C and C^*, and, finally, Eq. (5.6) describes diagrams D, E and F. A more detailed explanation is presented in Section 4.

Eqs. (5.4)-(5.8) can be written in a compact form as

$$\frac{\partial M_{lin}(12|12')}{\partial y}=\frac{\bar{\alpha_s}}{2\pi}\int d^2x_3\left\{-\frac{1}{2}\left(\frac{x_{13}}{x_{13}^2}-\frac{x_{23}}{x_{23}^2}\right)^2M_{lin}(12|12')-\frac{1}{2}\left(\frac{x_{13}}{x_{13}^2}-\frac{x_{2'3}}{x_{2'3}^2}\right)^2M_{lin}(12|12')\right. \tag{5.10}$$

$$+\left(\frac{x_{13}}{x_{13}^2}-\frac{x_{23}}{x_{23}^2}\right)\left(\frac{x_{13}}{x_{13}^2}-\frac{x_{2'3}}{x_{2'3}^2}\right)\{M_{lin}(13|13)+M_{lin}(32|32')\} \tag{5.11}$$

$$-\left(\frac{x_{13}}{x_{13}^2}-\frac{x_{23}}{x_{23}^2}\right)\left(\frac{x_{23}}{x_{23}^2}-\frac{x_{2'3}}{x_{2'3}^2}\right)M_{lin}(13|12')-\left(\frac{x_{2'3}}{x_{2'3}^2}-\frac{x_{23}}{x_{23}^2}\right)\left(\frac{x_{13}}{x_{13}^2}-\frac{x_{2'3}}{x_{2'3}^2}\right)M_{lin}(12|13)$$

$$-\frac{1}{2}\left(\frac{x_{23}}{x_{23}^2}-\frac{x_{2'3}}{x_{2'3}^2}\right)^2 M_{lin}(12|12')\Bigg\} \tag{5.12}$$

For $x_2 = x_{2'}$ all terms in Eqs. (5.12)-(5.12) cancel out and the linear evolution equation reduces to

$$\frac{\partial M_{lin}(12|12)}{\partial y}=\frac{\bar{\alpha_s}}{2\pi}\int d^2x_3\left(\frac{x_{13}}{x_{13}^2}-\frac{x_{23}}{x_{23}^2}\right)^2\left\{-\frac{2}{2}M_{lin}(12|12)+M_{lin}(13|13)+M_{lin}(32|32)\right\} \tag{5.13}$$

which is BFKL equation because of the unitarity condition $M_{lin}(12|12) = 2N_{lin}(12)$. As in the case of the non-linear equation it is easy to see from Eqs. (5.10)-(5.12) that its solution $M_{lin}(12|12')$ can be expressed through solution to BFKL equation as

$$M_{lin}(12|12') = N_{BFKL}(12) + N_{BFKL}(12') - N_{BFKL}(22') \tag{5.14}$$

This is a generalized form of the optical theorem, which relates the total cross section $M_{lin}(12|12')$ of scattering of the dipole "12"("12′") to the elastic scattering amplitude of the dipoles "12", "12′" and "$12-12'$".

We are interested in the contributions to the total cross section, which have different multiplicities as shown in Fig. 11

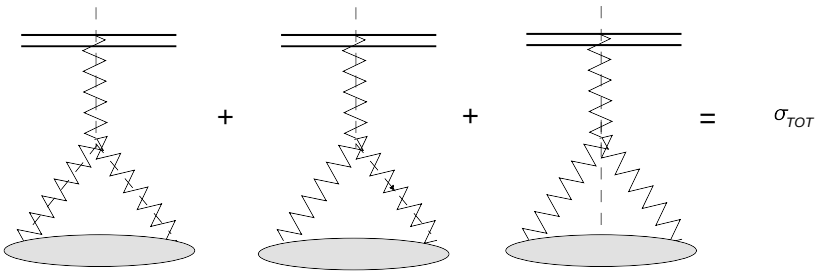

Figure 11: The contributions to the total cross section having different multiplicities.

We go back to the expression for the triple Pomeron vertex with interaction Eq. (5.3) and read out the contributions of the different cuts as follows.

$$\begin{array}{ll}
\text{Double Cut} & \frac{1}{2}\left(M_{lin}(12|12)+M_{lin}(20|20)\right)^2-\frac{1}{2}M_{lin}(10|10) \\
\text{Single Cut} & -\left(M_{lin}(12|12)+M_{lin}(20|20)\right)\left(2N_{\text{BFKL}}(12)+2N_{\text{BFKL}}(20)\right)+M_{lin}(10|10)2N_{\text{BFKL}}(10) \\
\text{Diffractive Cut} & \frac{2}{2}\left(N_{\text{BFKL}}(12)+N_{\text{BFKL}}(02)\right)^2-\frac{2}{2}N_{\text{BFKL}}^2(10)
\end{array} \tag{5.15}$$

One can easily see using the unitarity relation Eq. (5.14) $M_{lin}(ij|ij) = 2N_{\text{BFKL}}(ij)$ both the double and the single cut contributions are proportional to the diffractive term as expected from the AGK cutting rules.

$$\begin{aligned}
&\text{Double Cut} && 2\left(N_{\texttt{BFKL}}(12)+N_{\texttt{BFKL}}(02)\right)^2-2N^2_{\texttt{BFKL}}(10)\\
&\text{Single Cut} && -4\left(N_{\texttt{BFKL}}(12)+N_{\texttt{BFKL}}(02)\right)^2+4N^2_{\texttt{BFKL}}(10)\\
&\text{Diffractive Cut} && \left(N_{\texttt{BFKL}}(12)+N_{\texttt{BFKL}}(02)\right)^2-N^2_{\texttt{BFKL}}(10)
\end{aligned} \tag{5.16}$$

It is instructive to demonstrate how terms in Eq. (5.16) add up to the total cross section. The easiest way to see this is to write down the Glauber expression for the total cross section in Eq. (5.3) as follows

$$\sigma^{q\bar{q}}_{2P}(x_1,x_0)=\frac{\bar{\alpha}_s}{2\pi}\int_0^{Y_0}dy\int d^2x_2\left(\frac{x_{12}}{x^2_{12}}-\frac{x_{02}}{x^2_{02}}\right)^2\left\{2\left(1-e^{\frac{1}{2}(\sigma^{BA}(12)+\sigma^{BA}(20))}\right)-2\left(1-e^{\frac{1}{2}\sigma^{BA}(10)}\right)\right\}$$

where we used the notation of Appendix B and absorbed for simplicity $T(b;R_A)$ in the definition of σ^{BA}. The first term in the brackets in Eq. (5.17) is the total cross section of the scattering of $q\bar{q}g$ system after the soft gluon emission (dipole splitting) happened, this term comes from diagram A if Fig. 4. The second terms in Eq. (5.17) corresponds to the situation where the gluon is both emitted and absorbed before the scattering takes place (see diagrams R and R^* in Fig. 4). It is easy to see that the expansion of the expression in the brackets in Eq. (5.17) to the second order in σ^{BA} with the help of $\sigma^{BA}=2N^{BA}$ gives the sum of terms in Eq. (5.16).

The coefficients in Eq. (5.16) show that we fully reproduce the AGK cutting in this case. However, the situation changes when one emits a gluon from the triple Pomeron vertex. In this case the real-virtual cancellations does not happen and one should expect non-trivial contributions from different cuts as discussed in the next Section.

6. AGK rules for a production from vertex

In deriving the triple Pomeron vertex Eq. (5.3) we used the real-virtual cancellations, where the real gluon emissions were cancelled by the virtual emissions. This does not happen for the real gluon production (see Fig. 12) and we have to go back to extract only the real emission terms.

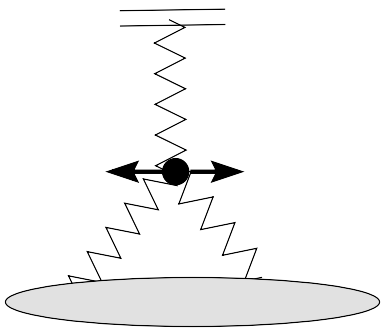

Figure 12: The emission from the vertex in one to two Pomerons splitting.

As in the case of no gluon production, this process can be written as

$$\frac{d\sigma}{dY_0\,d^2k}=\int P(Y-Y_0)\otimes\Gamma_{3P}(k,Y_0)\otimes P^2(Y_0-0) \tag{6.1}$$

where $P(Y-Y_0)$ is the Pomeron amplitude and Γ_{3P} is the triple Pomeron vertex with one gluon emission. In the case of the virtual photon scattering on the target this is given by

$$\frac{d\sigma}{dY_0\, d^2k} = \int d^2x_{\tilde{1}} d^2x_{\tilde{0}} d\tilde{z}\; d^2x_1 d^2x_0\; |\psi^{\gamma^*\to q\bar{q}}(x_{\tilde{1}\tilde{0}},\tilde{z})|^2 n_{lin}(x_{\tilde{1}},x_{\tilde{0}}|x_1,x_0;Y-Y_0)\frac{d\sigma_{2P}^{q\bar{q}}(x_1,x_0)}{dY_0 d^2k} \tag{6.2}$$

where $\psi^{\gamma^*\to q\bar{q}}(x_{\tilde{1}\tilde{0}},\tilde{z})$ is the wave function of the virtual photon being split into $q\bar{q}$ pair, $n_{lin}(x_{\tilde{1}},x_{\tilde{0}}|x_1,x_0,Y-Y_0)$ is the dipole density, which is the solution to the linear evolution equation.

All the information about the contributions of the different unitarity cuts is encoded in the differential cross section $\frac{d\sigma_{2P}^{q\bar{q}}(x_1,x_0)}{dY_0 d^2k}$. We can readily write it following the strategy we used before in deriving the single inclusive cross section Eqs. (3.2)-(3.6) in Section 3.

$$\begin{aligned}
\frac{d\sigma_{2P}^{q\bar{q}}(x_1,x_0)}{dY_0 d^2k} = \frac{\bar{\alpha}_s}{2\pi}\frac{1}{(2\pi)^2}\int d^2x_2\; d^2x_{2'} e^{-ik(x_2-x_{2'})}\left(\left(\frac{x_{12}}{x_{12}^2}-\frac{x_{02}}{x_{02}^2}\right)\left(\frac{x_{12'}}{x_{12'}^2}-\frac{x_{02'}}{x_{02'}^2}\right)\right.\{&\frac{1}{2}M_{lin}^2(12|12')+\frac{1}{2}M_{lin}^2(20|2'0) \\
+M_{lin}(12|12')M_{lin}(20|2'0)-(M_{lin}(12|12')+M_{lin}(20|2'0))&(N_{\text{BFKL}}(12)+N_{\text{BFKL}}(12')+N_{\text{BFKL}}(20)+N_{\text{BFKL}}(2'0)) \\
+N_{\text{BFKL}}(12)N_{\text{BFKL}}(2'0)+N_{\text{BFKL}}(20)N_{\text{BFKL}}(12')&+N_{\text{BFKL}}(12)N_{\text{BFKL}}(12')+N_{\text{BFKL}}(20)N_{\text{BFKL}}(2'0)\}
\end{aligned} \tag{6.3}$$

$$\begin{aligned}
&-\left(\frac{x_{12}}{x_{12}^2}-\frac{x_{02}}{x_{02}^2}\right)\left(0-\frac{x_{02'}}{x_{02'}^2}\right)\{-M_{lin}(12|10)\,(N_{\text{BFKL}}(20)+N_{\text{BFKL}}(12)+N_{\text{BFKL}}(10)) \\
&\qquad +\frac{1}{2}M_{lin}^2(12|10)+N_{\text{BFKL}}(12)N_{\text{BFKL}}(10)+N_{\text{BFKL}}(20)N_{\text{BFKL}}(10)\} \\
&-\left(\frac{x_{12}}{x_{12}^2}-\frac{x_{02}}{x_{02}^2}\right)\left(\frac{x_{12'}}{x_{12'}^2}-0\right)\{-M_{lin}(20|10)\,(N_{\text{BFKL}}(12)+N_{\text{BFKL}}(20)+N_{\text{BFKL}}(10)) \\
&\qquad +\frac{1}{2}M_{lin}^2(20|10)+N_{\text{BFKL}}(12)N_{\text{BFKL}}(10)+N_{\text{BFKL}}(20)N_{\text{BFKL}}(10)\} \\
&-\left(0-\frac{x_{02}}{x_{02}^2}\right)\left(\frac{x_{12'}}{x_{12'}^2}-\frac{x_{02'}}{x_{02'}^2}\right)\{-M_{lin}(10|12')\,(N_{\text{BFKL}}(2'0)+N_{\text{BFKL}}(12')+N_{\text{BFKL}}(10)) \\
&\qquad +\frac{1}{2}M_{lin}^2(10|12')+N_{\text{BFKL}}(10)N_{\text{BFKL}}(2'0)+N_{\text{BFKL}}(10)N_{\text{BFKL}}(12')\} \\
&-\left(\frac{x_{12}}{x_{12}^2}-0\right)\left(\frac{x_{12'}}{x_{12'}^2}-\frac{x_{02'}}{x_{02'}^2}\right)\{-M_{lin}(10|2'0)\,(N_{\text{BFKL}}(12')+N_{\text{BFKL}}(2'0)+N_{\text{BFKL}}(10)) \\
&\qquad +\frac{1}{2}M_{lin}^2(10|2'0)+N_{\text{BFKL}}(10)N_{\text{BFKL}}(2'0)+N_{\text{BFKL}}(10)N_{\text{BFKL}}(12')\}
\end{aligned}$$

$$\begin{aligned}
&+\left(\frac{x_{12}}{x_{12}^2}\frac{x_{12'}}{x_{12'}^2}+\frac{x_{02}}{x_{02}^2}\frac{x_{02'}}{x_{02'}^2}\right)\left\{\frac{1}{2}M_{lin}^2(10|10)-M_{lin}(10|10)2N_{\text{BFKL}}(10)+N_{\text{BFKL}}^2(10)\right\} \\
&-\left(\frac{x_{12}}{x_{12}^2}\frac{x_{02'}}{x_{02'}^2}+\frac{x_{02}}{x_{02}^2}\frac{x_{12'}}{x_{12'}^2}\right)N_{\text{BFKL}}^2(10)
\end{aligned}$$

We read out the double cut contribution from Eqs. (6.3)-(6.4)

$$\frac{d\sigma^{q\bar{q}}_{2P(double)}(x_1,x_0)}{dY_0 d^2k} = \frac{\bar{\alpha}_s}{2\pi}\frac{1}{(2\pi)^2}\int d^2x_2\; d^2x_{2'} e^{-ik(x_2-x_{2'})} \tag{6.4}$$
$$\Bigg(\frac{x_{12}}{x_{12}^2}\frac{x_{12'}}{x_{12'}^2}\frac{1}{2}\left\{(M^2_{lin}(12|12')+M^2_{lin}(20|2'0))^2 - M^2_{lin}(10|2'0) - M^2_{lin}(20|10) + M^2_{lin}(10|10)\right\}$$
$$+\frac{x_{02}}{x_{02}^2}\frac{x_{02'}}{x_{02'}^2}\frac{1}{2}\left\{(M^2_{lin}(12|12')+M^2_{lin}(20|2'0))^2 - M^2_{lin}(10|12') - M^2_{lin}(12|10) + M^2_{lin}(10|10)\right\}$$
$$-\frac{x_{12}}{x_{12}^2}\frac{x_{02'}}{x_{02'}^2}\frac{1}{2}\left\{(M^2_{lin}(12|12')+M^2_{lin}(20|2'0))^2 - M^2_{lin}(10|2'0) - M^2_{lin}(12|10)\right\}$$
$$+\frac{x_{02}}{x_{02}^2}\frac{x_{12'}}{x_{12'}^2}\frac{1}{2}\left\{(M^2_{lin}(12|12')+M^2_{lin}(20|2'0))^2 - M^2_{lin}(10|12') - M^2_{lin}(20|10)\right\}\Bigg)$$

It is a tedious, but a straightforward calculation to find the single cut contribution in the form of

$$\frac{d\sigma^{q\bar{q}}_{2P(single)}(x_1,x_0)}{dY_0 d^2k} = \frac{\bar{\alpha}_s}{2\pi}\frac{1}{(2\pi)^2}\int d^2x_2\; d^2x_{2'} e^{-ik(x_2-x_{2'})} \tag{6.5}$$
$$\Bigg(\frac{x_{12}}{x_{12}^2}\frac{x_{12'}}{x_{12'}^2}\{-\left(M_{lin}(12|12')+M_{lin}(20|2'0)\right)\left(N_{\text{BFKL}}(12)+N_{\text{BFKL}}(20)+N_{\text{BFKL}}(12')+N_{\text{BFKL}}(2'0)\right)$$
$$+M_{lin}(20|10)\left(N_{\text{BFKL}}(10)+N_{\text{BFKL}}(12)+N_{\text{BFKL}}(20)\right)+M_{lin}(10|2'0)\left(N_{\text{BFKL}}(10)+N_{\text{BFKL}}(12')+N_{\text{BFKL}}(2'0)\right)$$
$$-2M_{lin}(10|10)N_{\text{BFKL}}(10)\}$$
$$-\frac{x_{12}}{x_{12}^2}\frac{x_{02'}}{x_{02'}^2}\{-\left(M_{lin}(12|12')+M_{lin}(20|2'0)\right)\left(N_{\text{BFKL}}(12)+N_{\text{BFKL}}(20)+N_{\text{BFKL}}(12')+N_{\text{BFKL}}(2'0)\right)$$
$$+M_{lin}(12|10)\left(N_{\text{BFKL}}(10)+N_{\text{BFKL}}(12)+N_{\text{BFKL}}(20)\right)+M_{lin}(10|2'0)\left(N_{\text{BFKL}}(10)+N_{\text{BFKL}}(12')+N_{\text{BFKL}}(2'0)\right)\}$$
$$-\frac{x_{02}}{x_{02}^2}\frac{x_{12'}}{x_{12'}^2}\{-\left(M_{lin}(12|12')+M_{lin}(20|2'0)\right)\left(N_{\text{BFKL}}(12)+N_{\text{BFKL}}(20)+N_{\text{BFKL}}(12')+N_{\text{BFKL}}(2'0)\right)$$
$$+M_{lin}(20|10)\left(N_{\text{BFKL}}(10)+N_{\text{BFKL}}(12)+N_{\text{BFKL}}(20)\right)+M_{lin}(10|12')\left(N_{\text{BFKL}}(10)+N_{\text{BFKL}}(12')+N_{\text{BFKL}}(2'0)\right)\}$$
$$+\frac{x_{02}}{x_{02}^2}\frac{x_{02'}}{x_{02'}^2}\{-\left(M_{lin}(12|12')+M_{lin}(20|2'0)\right)\left(N_{\text{BFKL}}(12)+N_{\text{BFKL}}(20)+N_{\text{BFKL}}(12')+N_{\text{BFKL}}(2'0)\right)$$
$$+M_{lin}(12|10)\left(N_{\text{BFKL}}(10)+N_{\text{BFKL}}(12)+N_{\text{BFKL}}(20)\right)+M_{lin}(10|12')\left(N_{\text{BFKL}}(10)+N_{\text{BFKL}}(12')+N_{\text{BFKL}}(2'0)\right)$$
$$-2M_{lin}(10|10)N_{\text{BFKL}}(10)\}\Bigg)$$

Finally, the diffractive cut gives

$$\frac{d\sigma^{q\bar{q}}_{2P(diff)}(x_1,x_0)}{dY_0 d^2k} = \frac{\bar{\alpha}_s}{2\pi}\frac{1}{(2\pi)^2}\int d^2x_2\; d^2x_{2'} e^{-ik(x_2-x_{2'})}\left(\frac{x_{12}}{x_{12}^2}-\frac{x_{02}}{x_{02}^2}\right)\left(\frac{x_{12'}}{x_{12'}^2}-\frac{x_{02'}}{x_{02'}^2}\right) \tag{6.6}$$
$$\{N_{\text{BFKL}}(10)-N_{\text{BFKL}}(12)-N_{\text{BFKL}}(20)\}\{N_{\text{BFKL}}(10)-N_{\text{BFKL}}(12')-N_{\text{BFKL}}(2'0)\}$$

The contributions from the different cuts can be further simplified using the unitarity condition Eq. (5.14), but the expressions become cumbersome and we want to consider only a special case of $\frac{x_{12}}{x_{12}^2}\frac{x_{12'}}{x_{12'}^2}$ dipole splitting for illustrating the general conclusion regarding the AGK violation. The cuts are:

- **double cut**

$$\frac{1}{2}(4N^2_{\text{BFKL}}(10)-(N_{\text{BFKL}}(10)-N_{\text{BFKL}}(12)+N_{\text{BFKL}}(20))^2-(N_{\text{BFKL}}(10)-N_{\text{BFKL}}(12')+N_{\text{BFKL}}(2'0))^2 \tag{6.7}$$
$$+(N_{\text{BFKL}}(12)+N_{\text{BFKL}}(12')+N_{\text{BFKL}}(20)-2N_{\text{BFKL}}(22')+N_{\text{BFKL}}(2'0))^2)$$

- **single cut**

$$\begin{aligned} &-2(N^2_{\rm BFKL}(10)+N^2_{\rm BFKL}(12)+(N_{\rm BFKL}(12')+N_{\rm BFKL}(20))(N_{\rm BFKL}(12')-N_{\rm BFKL}(22')) \\ &+(N_{\rm BFKL}(12')+N_{\rm BFKL}(20)-N_{\rm BFKL}(22'))N_{\rm BFKL}(2'0)-N_{\rm BFKL}(10)(N_{\rm BFKL}(20)+N_{\rm BFKL}(2'0)) \\ &+N_{\rm BFKL}(12)(N_{\rm BFKL}(12')+N_{\rm BFKL}(20)-N_{\rm BFKL}(22')+N_{\rm BFKL}(2'0)) \end{aligned} \tag{6.8}$$

- **diffractive cut**

$$\{N_{\rm BFKL}(10)-N_{\rm BFKL}(12)-N_{\rm BFKL}(20)\}\{N_{\rm BFKL}(10)-N_{\rm BFKL}(12')-N_{\rm BFKL}(2'0)\} \tag{6.9}$$

It is clearly seen from Eqs. (6.7)-(6.9) that already in the single inclusive cross section the original AGK cutting rules are violated in the sense that the contributions from the different cuts are not proportional to each other. This should be compared to the cuts contributing to the total cross section given in Eq. (5.16), which are proportional to the total cross section with coefficients $2 \div -4 \div 1$.

It should be emphasized that, in contrary to the original AGK cutting rules, non of the cuts is expressed through the total cross section as we show in Appendix D.

In the production of another gluon from one of the lower Pomerons (see Fig. 13) one would expect a cancellation

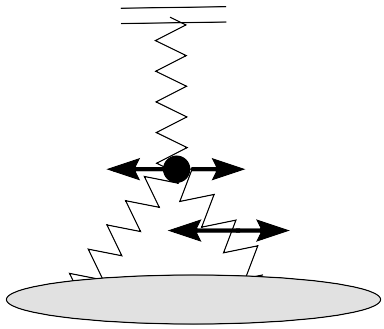

Figure 13: The emission from the vertex in one to two Pomerons splitting.

naively applying AGK cutting rules as shown Fig. 9. This does not happen if the gluon production is preceded by the emission from the vertex, because in this case the double cut Eq. (6.7) is not proportional to the single cut Eq. (6.8).

Another important remark is to be made, in the real gluon production from the vertex we took into account only diagrams A, B, B^* and D in Fig. 4. As we showed in Section 5 the cuts of diagram A fully satisfied the AGK rules for the total cross section, and we expect the AGK violation to originate only from diagram B, B^* and D in Fig. 4. This is not the case, because of the fact that the produced gluon transverse coordinate in the amplitude x_2 differs from its coordinate $x_{2'}$ in the conjugate amplitude. The cuts of diagram A in Fig. 4 for the dipole splitting $\frac{x_{12}}{x^2_{12}}\frac{x_{12'}}{x^2_{12'}}$ are given by

- **double cut of diagram** A

$$\frac{1}{2}\left(N_{\rm BFKL}(12)+N_{\rm BFKL}(12')+N_{\rm BFKL}(20)+N_{\rm BFKL}(2'0)-2N_{\rm BFKL}(22')\right)^2 \tag{6.10}$$

- **single cut of diagram A**

$$-\left(N_{\rm BFKL}(12)+N_{\rm BFKL}(12')+N_{\rm BFKL}(20)+N_{\rm BFKL}(2'0)\right)\left(N_{\rm BFKL}(12)+N_{\rm BFKL}(12')+N_{\rm BFKL}(20)+N_{\rm BFKL}(2'0)-2N_{\rm BFKL}(22')\right) \quad (6.11)$$

- **diffractive cut of diagram A**

$$+\left(N_{\rm BFKL}(12)+N_{\rm BFKL}(20)\right)\left(N_{\rm BFKL}(12')+N_{\rm BFKL}(2'0)\right) \quad (6.12)$$

The double Eq. (6.10), the single Eq. (6.11) and the diffractive Eq. (6.12) cuts are proportional to each other only for $x_2 = x_{2'}$.

Eq. (6.7) - Eq. (6.9) does not allow us to calculate the double inclusive cross section but we can easily to calculate the following observable $\int d^2k_1 d^2k_2 \int_0^{y_1} dy_2 d^6\sigma/d^2k_1 d^2k_2 dy_1 dy_2$ which gives the multiplicity of particles with rapidity less than y_1 which accompany the produced jet at rapidity y_1 integrated over possible transverse momentum. From Eq. (6.7) - Eq. (6.8) one can conclude that

$$\int d^2k_1 d^2k_2 \int_0^{y_1} dy_2 \; \frac{d^6\sigma}{d^2k_1 d^2k_2 dy_1 dy_2} \; = \quad (6.13)$$
$$\frac{\bar{\alpha}_S}{2\pi}\frac{1}{2\pi}\int d^2x_2 \; \frac{x_{01}^2}{x_{12}^2\, x_{02}^2}\, 4\, N_{\rm BFKL}(02)\; \left(N_{\rm BFKL}(01) \; - \; N_{\rm BFKL}(02) \; + \; N_{\rm BFKL}(12)\right)\; \langle |n(y_1-0)| \rangle_P$$

where $\langle |n(y_1-0)| \rangle_P$ is the average multiplicity in the rapidity window $y_1 - 0$.

One can see that cross section of Eq. (6.13) is not equal to zero and therefore, this equations confirms the main result of Ref. [10].

In the next Section we show processes of different multiplicity can be extracted directly from the Glauber expression for the single inclusive cross section.

7. AGK rules in Glauber Formalism

In this Section we use the Glauber expression for the single inclusive cross section including multiple rescatterings to find the contributions of different multiplicities to the total cross section. In the classical expression for the single inclusive cross section Eqs. (3.7)-(3.10) we included both elastic and inelastic rescatterings on a large target consisting of an infinite number of nucleons. In this Section we consider only two nucleons and show that in the leading order this coincides with the expression for two Pomeron exchange in Section 6. In order to do this we need to separate elastic and inelastic contributions in the Glauber expression Eqs. (3.7)-(3.10), since in its derivation we use cancellations of these two as follows. In Section 3 we started by defining cross section $M_0(ij|ik)$, which includes both elastic and inelastic parts and was found by Glauber summation in Appendix B. In passing from Eqs. (3.2)-(3.6) to Eqs. (3.7)-(3.10) we used Eq. (B-8) obtained from Eq. (B-5) with the help of Eq. (B-6). In this step we canceled some of the inelastic terms with the elastic ones. Our goal is to reconstruct the classical expression for the single inclusive cross section before we make use of these cancellations. To do this we just substitute the expression for the cross section $M_0(ij|ik)$ given by Eq. (B-5) in Eqs. (3.2)-(3.6).

After some lengthy calculations we obtain

$$\frac{d\sigma^{q\bar{q}A\to GX}(x_1,x_0)}{d^2k dy} = \frac{\bar{\alpha_s}}{2\pi}\frac{1}{(2\pi)^2}\int d^2x_2 d^2x_{2'} e^{-ik(x_2-x_{2'})}\left\{\left(\frac{x_{12}}{x_{12}^2}-\frac{x_{02}}{x_{02}^2}\right)\left(\frac{x_{12'}}{x_{12'}^2}-\frac{x_{02'}}{x_{02'}^2}\right)\right. \quad (7.1)$$

$$\left(1-e^{-\frac{1}{2}(\sigma^{BA}(12)+\sigma^{BA}(20))}-e^{-\frac{1}{2}(\sigma^{BA}(12')+\sigma^{BA}(2'0))}+e^{-\frac{1}{2}(\sigma^{BA}(12)+\sigma^{BA}(20)+\sigma^{BA}(12')+\sigma^{BA}(2'0))+\hat{\sigma}_{in}(12|12')+\hat{\sigma}_{in}(20|2'0)}\right) \quad (7.2)$$

$$\left.-\left(\frac{x_{12}}{x_{12}^2}-\frac{x_{02}}{x_{02}^2}\right)\left(0-\frac{x_{02'}}{x_{02'}^2}\right)\left(1-e^{-\frac{1}{2}(\sigma^{BA}(12)+\sigma^{BA}(20))}-e^{-\frac{1}{2}\sigma^{BA}(10)}+e^{-\frac{1}{2}(\sigma^{BA}(12)+\sigma^{BA}(20)+\sigma^{BA}(10))+\hat{\sigma}_{in}(12|10)}\right)\right. \quad (7.3)$$

$$
- \left(\frac{x_{12}}{x_{12}^2} - \frac{x_{02}}{x_{02}^2} \right) \left(\frac{x_{12'}}{x_{12'}^2} - 0 \right) \left(1 - e^{-\frac{1}{2}(\sigma^{BA}(12)+\sigma^{BA}(20))} - e^{-\frac{1}{2}\sigma^{BA}(10)} + e^{-\frac{1}{2}(\sigma^{BA}(12)+\sigma^{BA}(20)+\sigma^{BA}(10))+\hat{\sigma}_{in}(20|10)} \right)
$$

$$
- \left(0 - \frac{x_{02}}{x_{02}^2} \right) \left(\frac{x_{12'}}{x_{12'}^2} - \frac{x_{02'}}{x_{02'}^2} \right) \left(1 - e^{-\frac{1}{2}\sigma^{BA}(10)} - e^{-\frac{1}{2}(\sigma^{BA}(12')+\sigma^{BA}(2'0))} + e^{-\frac{1}{2}(\sigma^{BA}(12')+\sigma^{BA}(2'0)+\sigma^{BA}(10))+\hat{\sigma}_{in}(10|12')} \right)
$$

$$
- \left(\frac{x_{12}}{x_{12}^2} - 0 \right) \left(\frac{x_{12'}}{x_{12'}^2} - \frac{x_{02'}}{x_{02'}^2} \right) \left(1 - e^{-\frac{1}{2}\sigma^{BA}(10)} - e^{-\frac{1}{2}(\sigma^{BA}(12)+\sigma^{BA}(20))} + e^{-\frac{1}{2}(\sigma^{BA}(12')+\sigma^{BA}(2'0)+\sigma^{BA}(10))+\hat{\sigma}_{in}(10|2'0)} \right)
$$

$$
+ \left(\frac{x_{12}}{x_{12}^2} \frac{x_{12'}}{x_{12'}^2} + \frac{x_{02}}{x_{02}^2} \frac{x_{02'}}{x_{02'}^2} \right) \left(1 - 2\, e^{-\frac{1}{2}\sigma^{BA}(10)} + e^{-\frac{1}{2}2\sigma^{BA}(10)+\hat{\sigma}_{in}(10|10)} \right) - \left(\frac{x_{12}}{x_{12}^2} \frac{x_{02'}}{x_{02'}^2} + \frac{x_{02}}{x_{02}^2} \frac{x_{12'}}{x_{12'}^2} \right) \left(1 - e^{-\frac{1}{2}\sigma^{BA}(10)} \right)^2 \Big\} \quad (7.4)
$$

where, for simplicity, we absorbed the profile function $T(b; R_A)$ in the definition of the scattering cross sections σ^{BA} and $\hat{\sigma}_{in}$. The same expression can be directly applying Glauber formula as shown in Appendix D.

Now, we expand the exponentials Eqs. (7.1)-(7.4) in powers of $\hat{\sigma}^{in}$ to the second order to find the contributions that correspond to the double cut of two Pomeron exchange found in Eq. (6.4). After some algebra we obtain the same structure we have in Eq. (6.4). Expansion in powers of $(\sigma^{BA})^2$ reproduces the diffractive cut in Eq. (6.7), and, finally, the expansion in powers of $\hat{\sigma}^{in}\sigma^{BA}$ corresponds to the single cut in Eq. (6.5). It is important to note, that the classical expression in Eqs. (7.1)-(7.4) does not account for the evolution effects, and thus should not reproduce Eqs. (7.1)-(7.4) in more general case, when the evolution is switched on. The way to do this is to go back to Eqs. (3.2)-(3.6) and substitute solutions to the evolution equations $M(ij|ik)$ and $N(ij)$ in place of $M_0(ij|ik)$ and $N_0(ij)$ as described in Section 4. Then, expand to the desired order in $\hat{\sigma}_{in}$ and σ_{BA} to obtain contributions of different multiplicities. However, because of the fact that $M(ij|ik)$ and $N(ij)$ are solutions to non-linear equations with "Pomeron splittings" where "cut Pomeron" can split to two "uncut Pomerons" at some rapidity, fixing the interaction type ($\hat{\sigma}_{in}$ or σ_{BA}) by expanding the solution bring little or even no information about the multiplicity of the produced particles in the rapidity window between the target and the projectile. Thus, the proper way for studying the multiplicity distribution is to attach Pomerons (cut or uncut) to a triple Pomeron vertex at some given rapidity, as we did deriving Eqs. (6.3)-(6.4).

8. Conclusions

The central result of this paper is the proof of the validity of the Abramovsky-Gribov-Kancheli cutting rules in pQCD for the total cross section, and the demonstration of their violation for a particle production from the vertex. This violations happens already for one gluon production from the triple Pomeron vertex as shown by explicit calculation of contributions from different cuts to the inclusive cross section of two Pomeron exchange. The general conclusion can be formulated as follows: AGK rules valid for

- total cross section;
- production of any number of gluons from Pomerons either before or after triple Pomeron vertex.

AGK rules violated for

- one and more gluon productions from the triple Pomeron vertex.

This result allows to build a generating functional that will incorporate all multiparticle production processes in the spirit of Ref.[27], and find the equation for diffractive dissociation of Ref. [6].

As a by product of our analysis we derived a generalized form of the Balitsky-Kovchegov evolution equation for a non-diagonal cross section of the dipole scattering for a dipole having different coordinates in the amplitude and the conjugate amplitude. This generalised BK equation is easily solved by a linear combination of the solutions to the BK equation. This particular form of the solution preserves the adjoint (dipole) structure of the single inclusive cross section found by Kovchegov and Tuchin [9] to any order in the evolution.

The generalized BK equation found in the present paper is extremely useful for a systematic treatment of multigluon productions, multiparticle correlations including jet production in diffractive dissociation and multiplicity distributions in more general cases.

Acknowledgements

We are grateful to Jochen Bartels, Sergey Bondarenko, Errol Gotsman, Yura Kovchegov, Lev Lipatov, Cyrille Marquet, Uri Maor and Kirill Tuchin for fruitful discussions on the subject. Our special thanks go to Yura Kovchegov who found a mistake in the previous version of this paper which led us to an incorrect violation of Kovchegov-Tuchin formula for single inclusive cross section. One of us (A.P.) thanks Nestor Armesto and Carlos Pajares for their hospitality at University of Santiago de Compostela during the work of the paper. A.P. is also thankful to the organizers of the Les Houches School on Hadronic collisions 2008, in particular, to Yuri Dokshitzer, Francois Gelis and Edmond Iancu for their interest in the results of this study presented at the school.

This research was supported in part by the Israel Science Foundation, founded by the Israeli Academy of Science and Humanities, by BSF grant # 20004019 and by a grant from Israel Ministry of Science, Culture and Sport and the Foundation for Basic Research of the Russian Federation.

Appendices

A. Light Cone Perturbative QCD at high energy (simple diagrams)

In this Appendix we calculate simplest diagrams in the Light Cone Perturbation Theory (LCPT) applied to QCD, in particular, we show how the minus signs leading to the real-virtual cancellations appear in this framework. The rules for LCPT in QCD were formulated Ref. [19]. LCPT is very useful for high energy scattering since it represents an intuitive space-time picture of the scattering process. As a simple example of LCPT calculations consider a diagram where a soft gluon k is emitted from the heavy quark, and then the heavy quark interacts with the target as shown in Fig. 14. The interaction with the target is mediated by the gluon m and the intermediate states are denoted by the vertical dotted lines with light-cone energy denominators D_1 and D_2 are calculated from

$$D = \sum_i p^i_- - \sum_f p^f_- \tag{A-1}$$

where $\sum_i p^i_-$ and $\sum_f p^f_-$ are the sums of the light-cone energies of the intermediate and the initial (or equivalently final) states, correspondingly. The denominators D_1 and D_2 are readily found using Eq. (A-1)

$$D_1 = (p-k)_- + k_- + P_- - p_- - P_- = \frac{(p-k)^2_\perp}{(p-k)_+} + \frac{k^2_\perp}{k_+} + \frac{p^2_\perp}{p_+} \simeq \frac{k^2_\perp}{k_+} = k_- \tag{A-2}$$

$$D_2 = (p-k-m)_- + k_- + m_- + P_- - p_- - P_- = \frac{(p-k-m)^2_\perp}{(p-k-m)_+} + \frac{k^2_\perp}{k_+} + \frac{m^2_\perp}{m_+} + \frac{p^2_\perp}{p_+} \simeq \frac{k^2_\perp}{k_+} \simeq \frac{m^2_\perp}{m_+} = m_- \tag{A-3}$$

where we used the fact that $p_+ \gg k_+ \gg m_+$ in accordance with the Regge kinematics.

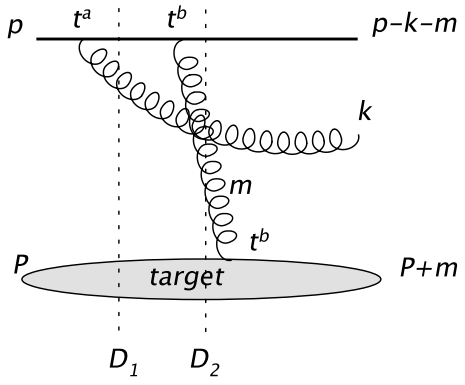

Figure 14: Emission of gluon in Light Cone Perturbative QCD .

The expression for the diagram depicted in Fig. 14 is given by

$$\frac{\bar{u}(P+m)}{\sqrt{(P+m)_+}} g t^b \gamma^\lambda \frac{u(P)}{\sqrt{(P)_+}} \frac{1}{D_2} \frac{g^{\mu\lambda}}{m_+} \frac{\bar{u}(p-k-m)}{\sqrt{(p-k-m)_+}} g t^b \gamma^\mu \frac{u(p-k)}{\sqrt{(p-k)_+}} \frac{1}{D_1} \frac{\bar{u}(p-k)}{\sqrt{(p-k)_+}} g t^a \gamma^\nu \frac{u(p)}{\sqrt{p_+}} \tag{A-4}$$

After some simplifications due to the normalization properties of the spinors in the kinematic regime $p_+ \gg k_+ \gg m_+$ we obtain

$$4g^2 t^b \otimes t^b \frac{1}{m_\perp^2} 2gt^a \frac{\epsilon_-}{k_-} = 4g^2 t^b \otimes t^b \frac{1}{m_\perp^2} 2gt^a \frac{k_\perp \cdot \epsilon_\perp}{k_\perp^2} \tag{A-5}$$

where we used the fact that $\epsilon \cdot k = 0 = \epsilon_+ k_- + \epsilon_- k_+ - \epsilon_\perp \cdot k_\perp \simeq \epsilon_- k_+ - \epsilon_\perp \cdot k_\perp$.

Next, we calculate the so-called late emission diagram where the emission of the gluon k occurs after the interaction as shown in Fig. 15

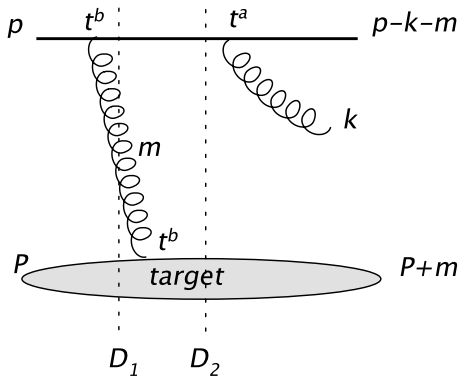

Figure 15: Late emission diagram in LCPT. This diagram is opposite in sign w.r.t the early emission in Fig. 14

As in the case of Fig. 14 we write the light-cone energy denominators

$$D_1 = (p-m)_- + m_- + P_- - p_- - P_- = \frac{(p-m)_\perp^2}{(p-m)_+} + \frac{m_\perp^2}{m_+} + \frac{p_\perp^2}{p_+} \simeq \frac{m_\perp^2}{m_+} = m_- \tag{A-6}$$

$$D_2 = (p-m)_- + m_- + (P+m)_- - (p-k-m)_- - (P+m)_- - k_- \simeq -k_- \tag{A-7}$$

In Eq. (A-7) we used the equivalence of the initial and the final light-cone energies. Note that due to the presence of the emitted gluon k in the final state D_2 generates a minus sign. The rest of the calculation is straightforward and in full analogy with Eq. (A-4). The final answer for the late emission diagram in Fig. 15 is given by

$$-4g^2 t^b \otimes t^b \frac{1}{m_\perp^2} 2gt^a \frac{\epsilon_-}{k_-} = 4g^2 t^b \otimes t^b \frac{1}{m_\perp^2} 2gt^a \frac{k_\perp \cdot \epsilon_\perp}{k_\perp^2} \tag{A-8}$$

and differs from Eq. (A-5) only by a minus sign coming from the light-cone energy denominator Eq. (A-7).

Here we presented a simplified case only one quark scattered off the target. In general, any late emission diagram will generate a minus sign w.r.t early emissions.

B. Calculation of $M_0(il|kl)$

In this Appendix we derive the explicit expression for $M_0(il|kl)$ for dipole-nucleus scattering in the Glauber approach assuming the Born Approximation of perturbative QCD (the exchange of two Coulomb-like gluons) for the dipole-nucleon interaction. It is well known that the Glauber formula for the imaginary part of the scattering amplitude in

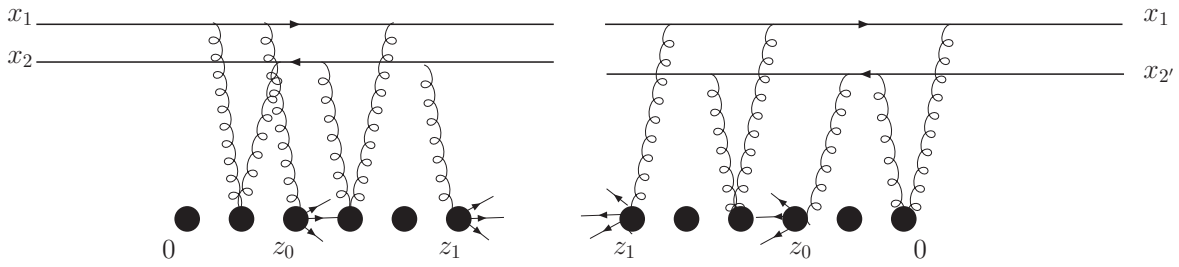

Figure 16: Amplitude $M_0\,(12|12')$ in Glauber approach.

this case has the following form

$$N_0(10) \;=\; 1 \;-\; e^{-\frac{1}{2}\sigma^{BA}(x_{10}^2)\,T(b;R_A)} \tag{B-1}$$

with

$$\sigma^{BA}(10) \;\equiv\; \sigma^{BA}(x_{10}) \;=\; 2\,\bar{\alpha}_S \int \frac{d^2l}{l^2}\,\left(1 \;-\; e^{-il\cdot x_{10}}\right)\,IF(l) \tag{B-2}$$

where l is the transverse momentum of one of two gluons in the Born Approximation diagram.

The function $IF(l)$ in Eq. (B-2) denotes so-called impact factor and describes the interaction of two gluon with a nucleon which depends on l^2. In our further calculations we do not need to know the explicit form of $IF(l)$.

The profile function $T\,(b;R_A)$ determines the number nucleons that can interact with the dipole at a given impact parameter $\vec{b} = \frac{1}{2}(\vec{x}_1 + \vec{x}_0)$. The profile function $T\,(b;R_A)$ is defined through the nucleon density in a nucleus $\rho(b,z)$ as

$$T\,(b;R_A) \;=\; \int dz\,\rho(b,z); \qquad \int d^2b \int_{-\infty}^{+\infty} dz\;\rho(b,z) \;=\; A \tag{B-3}$$

In the simple model $\rho(b,z) \;=\; \rho_0\,\Theta\,(R_A - b)\;\Theta\left(\sqrt{R_A^2 - b^2} - z\right)$, where R_A is the nucleus radius.

Let us consider a dipole having different sizes at the interaction time $\tau = 0$ in the amplitude and conjugate amplitude, namely, a dipole with quark (antiquark) coordinates x_1 (x_2) at $\tau = 0$ in amplitude and x_1 $(x_{2'})$ in the conjugate amplitude. A more general case with all the coordinates being different is of no use in our derivation and thus will be omitted. The cross section $M(12|12')$ is normalized such that $M(12|12) \;=\; 2\,N(12)$.

As one can see in Fig. 16 the interaction of the dipole "12" as well as the dipole "12′" with a nucleus includes an additional elastic rescattering as well as the inelastic interaction with the nucleons of the nucleus at points z_i.

To include both of the processes we first write the formula that sums all possible inelastic interactions. It has the form of [29, 28]

$$M_0^{in}\,(12|12') = \tag{B-4}$$
$$\times \int_0^{2R_A(b)} \rho\,\hat{\sigma}_{in}(12|12')\,dz_0\,e^{-\frac{1}{2}(\sigma^{BA}(12)+\sigma^{BA}(12'))\,\rho\,2\,R_A(b)} \sum_{n=0}^{\infty} \int_{z_0}^{2R_A(b)} d\,z_1\;\ldots \int_{z_{n-2}}^{2R_A(b)} dz_{n-1} \int_{z_{n-1}}^{2R_A(b)} dz_n\,\rho^n\,\hat{\sigma}_{in}^n(12|12')$$

The factor of $\exp\left(-\frac{1}{2}(\sigma(12)+\sigma(12'))\,\rho\,2\,R_A(b)\right)$ in Eq. (B-4)describes the fact that there are no inelastic interactions between points $z_1, z_2 \ldots z_n$. Any of the inelastic interactions occurs with the same nucleon in amplitude and conjugated amplitude since the contributions of the inelastic processes with different nucleons can be expressed

through the nucleon correlations in the nucleus which are suppressed in heavy nuclei. The sum in Eq. (B-4) exponentiates and gives

$$M_0^{in}\,(12|12')\;=\Big(e^{+\hat{\sigma}_{in}(12|12')\;T(b;R_A)}\;\;-\;\;1\Big)\,e^{-\frac{1}{2}\left\{\sigma^{BA}(12)+\sigma^{BA}(12')\right\}\,T(b;R_A)} \tag{B-5}$$

$$\begin{aligned}\hat{\sigma}_{in}(12|12') \;\;&=\;\;2\int\frac{d^2l}{l^2}\,\left(1\;-\;e^{-il\cdot x_{12}}\right)\times\left(1\;-\;e^{-il\cdot x_{12'}}\right)\,IF(l)\\ &=\;\;\frac{1}{2}\,\left(\sigma^{BA}(12)+\sigma^{BA}(12')\;-\;\sigma^{BA}(22')\right) \qquad\text{(B-6)}\\ \text{where }\sigma^{BA}(22')\;&=\;\sigma^{BA}(|\vec{x}_{12}-\vec{x}_{12'}|) \qquad\text{(B-7)}\end{aligned}$$

Using Eq. (B-6) and Eq. (B-7) we can reduce Eq. (B-5) to

$$M_0^{in}\,(12|12')\;=\;e^{-\frac{1}{2}\,\sigma^{BA}(22')\;T(b;R_A)}\;\;-\;\;e^{-\frac{1}{2}\left\{\sigma^{BA}(12)+\sigma^{BA}(12')\right\}\,T(b;R_A)} \tag{B-8}$$

To obtain the final formula we need to add to Eq. (B-8) the contribution of the elastic scattering which has the obvious form

$$M_0^{el}\,(12|12')\;=\;\left(1\;-\;e^{-\frac{1}{2}\,\sigma^{BA}(12)\;T(b;R_A)}\right)\times\left(1\;-\;e^{-\frac{1}{2}\,\sigma^{BA}(12')\;T(b;R_A)}\right) \tag{B-9}$$

Following the lines of Refs. [8, 18] we use the explicit expression for the powers of the exponentials in Eq. (B-8) and Eq. (B-9), namely,

$$\frac{1}{2}\,\sigma^{BA}(12)\;T\,(b;R_A)=\frac{1}{4}x_{12}^2Q_s^2 \tag{B-10}$$

where Q_s is the saturation scale used in the McLerran-Venugopalan model [3, 29, **?**] defined as

$$Q_s^2(b)=2\alpha_s\rho T(b) \tag{B-11}$$

Using this simple notation we can readily find from Eq. (B-8) and Eq. (B-9)

$$M_0(12|12')\;\;=\;\;1+e^{-x_{22'}^2Q_s^2/4}-e^{-x_{12}^2Q_s^2/4}-e^{-x_{12'}^2Q_s^2/4} \tag{B-12}$$

$$M_0(12|10)\;=\;1+e^{-x_{20}^2Q_s^2/4}-e^{-x_{12}^2Q_s^2/4}-e^{-x_{10}^2Q_s^2/4} \tag{B-13}$$

$$M_0(10|10)\;=\;2(1-e^{-x_{10}^2Q_{s0}^2/4}) \tag{B-14}$$

and other required combinations.

C. First step of the evolution in the Glauber approach

In this section we consider the first step of the evolution for the dipole "12"("12′") having different transverse coordinates in the amplitude and the conjugate amplitude, namely, we emit one extra soft gluon "3" as depicted in Fig. 7. The evolution in this case is described by the equation Eqs. (4.1) -(4.6) and its first iteration gives the

required emission of soft gluon "3". We analyze this situation both using Eqs. (4.1) -(4.6) and show its equivalence to the direct application of the Glauber theory.

The soft gluon "3" can be emitted before or after the interaction time $\tau = 0$. Firstly, we consider the contribution of the diagram A in Fig. 7 where the soft gluon is emitted before $\tau = 0$ in both the amplitude and the conjugate amplitude. The direct application of the Glauber expressions for the scattering cross section of two dipoles "13" and "32"("32′") found in Appendix B gives in this case

$$\begin{aligned}&\overbrace{\left(1-e^{-(x_{13}^2+x_{32}^2)Q_s^2/4}\right)\left(1-e^{-(x_{13}^2+x_{32'}^2)Q_s^2/4}\right)}^{\text{elastic scattering in the amplitude and conjugated amplitude}} \quad + \quad \overbrace{e^{-x_{22'}^2Q_s^2/4}-e^{-(2x_{13}^2+x_{32}^2+x_{32'}^2)Q_s^2/4}}^{\text{inelastic scattering in the amplitude and conjugated amplitude}} \\ &= 1+e^{-x_{22'}^2Q_s^2/4}-e^{-(x_{13}^2+x_{32}^2)Q_s^2/4}-e^{-(x_{13}^2+x_{32'}^2)Q_s^2/4}\end{aligned} \tag{C-1}$$

times the Kernel of the dipole splitting (the emission soft gluon "3") given by

$$\frac{\bar{\alpha_s}}{2\pi}\left(\frac{x_{13}}{x_{13}^2}-\frac{x_{23}}{x_{23}^2}\right)\left(\frac{x_{13}}{x_{13}^2}-\frac{x_{2'3}}{x_{2'3}^2}\right) \tag{C-2}$$

On the other hand we can use Eq. (4.2) and Eq. (4.3) to obtain the same result as follows

$$\begin{aligned}&M_0(13|13)+M_0(32|32')+M_0(13|13)M_0(32|32')-2M_0(32|32')N_0(13) \\ &-M_0(13|13)\left\{N_0(32)+N_0(32')\right\}+N_0(13)\left\{N_0(32')+N_0(32)\right\} \\ &=2\left(1-e^{-x_{13}^2Q_s^2/4}\right)+\left(1+e^{-x_{22'}^2Q_s^2/4}-e^{-x_{32}^2Q_s^2/4}-e^{-x_{32'}^2Q_s^2/4}\right) \\ &2\left(1-e^{-x_{13}^2Q_s^2/4}\right)\left(1+e^{-x_{22'}^2Q_s^2/4}-e^{-x_{32}^2Q_s^2/4}-e^{-x_{32'}^2Q_s^2/4}\right) \\ &-2\left(1+e^{-x_{22'}^2Q_s^2/4}-e^{-x_{32}^2Q_s^2/4}-e^{-x_{32'}^2Q_s^2/4}\right)\left(1-e^{-x_{13}^2Q_s^2/4}\right) \\ &-2\left(1-e^{-x_{13}^2Q_s^2/4}\right)\left(1-e^{-x_{32}^2Q_s^2/4}+1-e^{-x_{32'}^2Q_s^2/4}\right) \\ &+\left(1-e^{-x_{13}^2Q_s^2/4}\right)\left(1-e^{-x_{32}^2Q_s^2/4}+1-e^{-x_{32'}^2Q_s^2/4}\right) \\ &=2\left(1-e^{-x_{13}^2Q_s^2/4}\right)+\left(1+e^{-x_{22'}^2Q_s^2/4}-e^{-x_{32}^2Q_s^2/4}-e^{-x_{32'}^2Q_s^2/4}\right) \\ &-\left(1-e^{-x_{13}^2Q_s^2/4}\right)\left(1-e^{-x_{32}^2Q_s^2/4}+1-e^{-x_{32'}^2Q_s^2/4}\right) \\ &=1+e^{-x_{22'}^2Q_s^2/4}-e^{-(x_{13}^2+x_{32}^2)Q_s^2/4}-e^{-(x_{13}^2+x_{32'}^2)Q_s^2/4}\end{aligned} \tag{C-3}$$

In the limit of $x_2 = x_{2'}$ this equals to the total cross section of the two dipole scattering $2(1-e^{-(x_{13}^2+x_{32}^2)Q_s^2/4})$ as expected from the optical theorem.

Next, we want to obtain the contribution of diagram B in Fig. 7. The direct application of the Glauber formulae gives

$$\begin{aligned}&\overbrace{\left(1+e^{-(x_{13}^2+x_{32}^2)Q_s^2/4}\right)\left(1+e^{-x_{12'}^2Q_s^2/4}\right)}^{\text{elastic scattering in the amplitude and conjugated amplitude}} \quad + \quad \overbrace{e^{-(x_{32}^2+x_{32'}^2)Q_s^2/4}-e^{-(2x_{13}^2+x_{32}^2+x_{32'}^2)Q_s^2/4}}^{\text{inelastic scattering in the amplitude and conjugated amplitude}} \\ &= 1+e^{-(x_{32}^2+x_{32'})Q_s^2/4}-e^{-(x_{13}^2+x_{32}^2)Q_s^2/4}-e^{-x_{12'}^2Q_s^2/4}\end{aligned} \tag{C-4}$$

The same result one obtains using Eq. (4.4) in the evolution equation for $M(12|12')$ and the eikonal formulae for one dipole scattering

$$
\begin{aligned}
&M_0(13|12')\left\{1-N_0(32)\right\}+N_0(12')N_0(32) \qquad \text{(C-5)}\\
&=\left(1+e^{-x^2_{32'}Q_s^2/4}-e^{-x^2_{13}Q_s^2/4}-e^{-x^2_{12'}Q_s^2/4}\right)\left(1-1+e^{-x^2_{32}Q_s^2/4}\right)+\left(1-e^{-x^2_{12'}Q_s^2/4}\right)\left(1-e^{-x^2_{32}Q_s^2/4}\right)\\
&=1+e^{-(x^2_{32}+x_{32'})Q_s^2/4}-e^{-(x^2_{13}+x^2_{32})Q_s^2/4}-e^{-x^2_{12'}Q_s^2/4}
\end{aligned}
$$

The contribution from diagram B^* is found in analogous way.

The remaining diagrams R, R^*, D, E and F change the cross section merely by multiplication of the Kernel of the emission of the soft gluon "3", in other words, when gluon "3" is emitted in those diagrams, only the initial dipole interacts with the target as

$$
M_0(12|12')=1+e^{-x^2_{22'}Q_s^2/4}-e^{-x^2_{12}Q_s^2/4}-e^{-x^2_{12'}Q_s^2/4} \qquad \text{(C-6)}
$$

In this way we show that evolution equation Eqs. (4.8)-(4.11), correctly describe the evolution to the first order. The higher order iterations can be found in the same way.

D. Glauber expression for single inclusive cross section: AGK cuts

In this Appendix we show how the Glauber expression for the single inclusive cross section with inelastic part retained found in Section 7 (see Eqs. (7.1)-(7.4)) can be obtained directly applying the Glauber formula. The cross section for single inclusive production consists of terms coming from diagram A in Fig. 4(see Eq. (7.3)), diagrams B and B^* (see Eq. (7.4)) and diagram D (see Eq. (7.4)). We follow the lines of the Appendix C and readily write the Glauber expression for diagram A in Fig. 4 as

$$
\begin{aligned}
&\overbrace{\left(1-e^{-\frac{1}{2}\{\sigma^{BA}(12)+\sigma^{BA}(20)\}}\right)\left(1-e^{-\frac{1}{2}\{\sigma^{BA}(12')+\sigma^{BA}(2'0)\}}\right)}^{\text{elastic scattering in the amplitude and conjugated amplitude}} \qquad \text{(D-1)}\\
&+\overbrace{e^{-\frac{1}{2}\{\sigma^{BA}(12)+\sigma^{BA}(20)+\sigma^{BA}(12')+\sigma^{BA}(2'0)\}}-e^{-\frac{1}{2}\{\sigma^{BA}(12)+\sigma^{BA}(20)+\sigma^{BA}(12')+\sigma^{BA}(2'0)\}+\hat{\sigma}_{in}(12|12')+\hat{\sigma}_{in}(20|2'0)}}^{\text{inelastic scattering in the amplitude and conjugated amplitude}}\\
&=1-e^{-\frac{1}{2}\{\sigma^{BA}(12)+\sigma^{BA}(20)\}}-e^{-\frac{1}{2}\{\sigma^{BA}(12')+\sigma^{BA}(2'0)\}}\\
&\quad -e^{-\frac{1}{2}\{\sigma^{BA}(12)+\sigma^{BA}(20)+\sigma^{BA}(12')+\sigma^{BA}(2'0)\}+\hat{\sigma}_{in}(12|12')+\hat{\sigma}_{in}(20|2'0)}
\end{aligned}
$$

where we kept $2\neq 2'$ (coordinate of gluon in the amplitude and the conjugate amplitude) because we fix the momentum of the emitted gluon, and absorbed $T(b;R_A)$ in the definition of σ^{BA}. In the diagram A in Fig. 4 we depicted only $\frac{x_{12}}{x^2_{12}}\frac{x_{12'}}{x^2_{12'}}$ splitting, all other kernel have the same Glauber expression. This is not the case as far diagrams of the type B, B^* and D are concerned, their Glauber expression depend on the dipole splitting, since some inelastic contributions are suppressed in large N_C limit. We have already discussed this point deriving the single inclusive

cross section Eqs.(3.2)-(3.6) in Section 3. The diagram B, as it is shown in Fig. 4, brings

$$\overbrace{\left(1-e^{-\frac{1}{2}\{\sigma^{BA}(12)+\sigma^{BA}(20)\}}\right)\left(1-e^{-\frac{1}{2}\sigma^{BA}(10)}\right)}^{\text{elastic scattering in the amplitude and conjugated amplitude}} \tag{D-2}$$
$$+\overbrace{e^{-\frac{1}{2}\{\sigma^{BA}(12)+\sigma^{BA}(20)+\sigma^{BA}(10)\}}-e^{-\frac{1}{2}\{\sigma^{BA}(12)+\sigma^{BA}(20)+\sigma^{BA}(10)\}+\hat{\sigma}_{in}(12|10)}}^{\text{inelastic scattering in the amplitude and conjugated amplitude}}$$
$$=1-e^{-\frac{1}{2}\{\sigma^{BA}(12)+\sigma^{BA}(20)\}}-e^{-\frac{1}{2}\sigma^{BA}(10)}-e^{-\frac{1}{2}\{\sigma^{BA}(12)+\sigma^{BA}(20)+\sigma^{BA}(10)\}+\hat{\sigma}_{in}(12|10)}$$

All other splittings for type B diagrams are found in a similar way by replacing $\hat{\sigma}_{in}(12|10)$ by the proper inelastic term, same for B^*. The term resulting from diagram D in Fig. 4 is readily calculated as

$$\overbrace{\left(1-e^{-\frac{1}{2}\sigma^{BA}(10)}\right)\left(1-e^{-\frac{1}{2}\sigma^{BA}(10)}\right)}^{\text{elastic scattering in the amplitude and conjugated amplitude}} \tag{D-3}$$
$$+\overbrace{e^{-\frac{1}{2}2\sigma^{BA}(10)}-e^{-\frac{1}{2}2\sigma^{BA}(10)+\hat{\sigma}_{in}(10|10)}}^{\text{inelastic scattering in the amplitude and conjugated amplitude}}$$
$$=1-e^{-\frac{1}{2}\sigma^{BA}(10)}-e^{-\frac{1}{2}\sigma^{BA}(10)}-e^{-\frac{1}{2}2\sigma^{BA}(10)+\hat{\sigma}_{in}(10|10)}$$

The crossed dipole splittings $\frac{x_{12}}{x_{12}^2}\frac{x_{02'}}{x_{02'}^2}$ and $\frac{x_{02}}{x_{02}^2}\frac{x_{12'}}{x_{12'}^2}$ in D-type diagrams, has inelastic cross section suppressed in the large N_C limit giving just the elastic term. One can see that this way we reproduce the single inclusive cross section in the Glauber form Eqs. (7.1)-(7.4) found from a general expression Eqs. (3.2)-(3.5).

References

[1] L. V. Gribov, E. M. Levin and M. G. Ryskin, *Phys. Rep.* **100**, 1 (1983).

[2] A. H. Mueller and J. Qiu, *Nucl. Phys.* **B 268** 427 (1986) .

[3] L. McLerran and R. Venugopalan, *Phys. Rev.* **D 49**,2233, 3352 (1994); **D 50**,2225 (1994); **D 53**,458 (1996); **D 59**,09400 (1999).

[4] A. H. Mueller, *Nucl. Phys.* **B415**, 373 (1994); *ibid* **B437**, 107 (1995).

[5] V. A. Abramovsky, V. N. Gribov and O. V. Kancheli, Yad. Fiz. **18**, 595 (1973) [Sov. J. Nucl. Phys. **18**, 308 (1974)].

[6] Y. V. Kovchegov and E. Levin, Nucl. Phys. B **577** (2000) 221 [arXiv:hep-ph/9911523].

[7] M. Salvadore, J. Bartels and G. P. Vacca, *"Multiple interactions and AGK rules in pQCD,"* arXiv:0709.3062 [hep-ph]; F. Gelis and R. Venugopalan, Nucl. Phys. A **782** (2007) 297, **785** (2007) 146], [arXiv:hep-ph/0608117]; J. Bartels, M. Salvadore and G. P. Vacca, Eur. Phys. J. C **42** (2005) 53 [arXiv:hep-ph/0503049]; J. Bartels and M. G. Ryskin, Z. Phys. C **76** (1997) 241 [arXiv:hep-ph/9612226]; D. Treleani, Int. J. Mod. Phys. A **11** (1996) 613.

[8] Y. V. Kovchegov, Phys. Rev. D **64**, 114016 (2001) [Erratum-ibid. D **68**, 039901 (2003)] [arXiv:hep-ph/0107256].

[9] Y. V. Kovchegov and K. Tuchin, Phys. Rev. D **65**, 074026 (2002) [arXiv:hep-ph/0111362].

[10] J. Jalilian-Marian and Y. V. Kovchegov, Phys. Rev. D **70**, 114017 (2004) [Erratum-ibid. D **71**, 079901 (2005)] [arXiv:hep-ph/0405266].

[11] M. A. Braun, Eur. Phys. J. C **48**, 501 (2006) [arXiv:hep-ph/0603060].

[12] C. Marquet, Nucl. Phys. B **705**, 319 (2005) [arXiv:hep-ph/0409023].

[13] A. Kovner and M. Lublinsky, JHEP **0611**, 083 (2006) [arXiv:hep-ph/0609227].

[14] Z. Chen and A. H. Mueller, Nucl. Phys. B **451**, 579 (1995).

[15] E. A. Kuraev, L. N. Lipatov, and F. S. Fadin, *Sov. Phys. JETP* **45**, 199 (1977); Ya. Ya. Balitsky and L. N. Lipatov, *Sov. J. Nucl. Phys.* **28**, 22 (1978).

[16] J. Bartels, M. Salvadore and G. P. Vacca, arXiv:0802.2702 [hep-ph].

[17] I. Balitsky, [arXiv:hep-ph/9509348]; *Phys. Rev.* **D60**, 014020 (1999) [arXiv:hep-ph/9812311]

[18] Y. V. Kovchegov, *Phys. Rev.* **D60**, 034008 (1999), [arXiv:hep-ph/9901281].

[19] G. P. Lepage and S. J. Brodsky, Phys. Rev. D **22**, 2157 (1980).

[20] HighEnergy Particle Diffraction, V. Barone & E. Predazzi, Springer 2002

[21] M. A. Braun, Eur. Phys. J. C **39**, 451 (2005) [arXiv:hep-ph/0410164].

[22] M. A. Braun, Eur. Phys. J. C **42**, 169 (2005) [arXiv:hep-ph/0502184].

[23] M. A. Braun, arXiv:0801.0493 [hep-ph].

[24] J. Bartels and K. Kutak, Eur. Phys. J. C **53** (2008) 533 [arXiv:0710.3060 [hep-ph]].

[25] E. M. Levin and M. G. Ryskin, Yad. Fiz. **45** (1987) 234 [Sov. J. Nucl. Phys. **45** (1987) 150].

[26] D. Amati, A. Stanghellini and S. Fubini, Nuovo Cim. **26** (1962) 896.

[27] E. Levin and A. Prygarin, Eur. Phys. J. C **53** (2008) 385 [arXiv:hep-ph/0701178].

[28] Y. V. Kovchegov and A. H. Mueller, Nucl. Phys. B **529** (1998) 451 [arXiv:hep-ph/9802440].

[29] E. M. Levin and M. G. Ryskin, Yad. Fiz. **33** (1981) 1673; .